

A Project- II report on

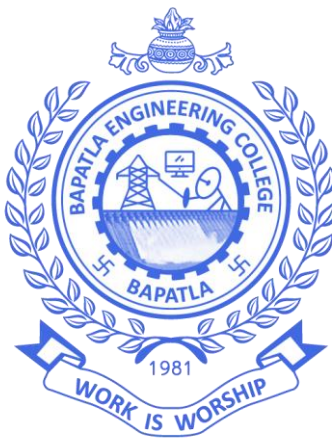
**EXPERIMENTAL INVESTIGATION ON TOOL VIBRATIONS  
DURING SURFACE DEFECTIVE MILLING OF ZK60/ B<sub>4</sub>C / Al<sub>2</sub>O<sub>3</sub>  
HYBRID METAL MATRIX COMPOSITES.**

Submitted in partial fulfilment of the requirement for the Degree of  
Bachelor of Technology  
in  
Mechanical Engineering.

Submitted by

KORAMUTLA SAI RAM [L20AME502]  
KOMMANAMANCHI KAMALAKAR [L20AME498]  
KHANDAVALLI HEMANTH [L20AME496]  
MARUPU DEVARAJ [L20AME516].

Under the guidance of  
Dr B. RAVI SANKAR  
Professor, Department of Mechanical Engineering.



**DEPARTMENT OF MECHANICAL ENGINEERING  
BAPATLA ENGINEERING COLLEGE: BAPATLA  
(AUTONOMOUS)  
(2022-2023)**

**BAPATLA ENGINEERING COLLEGE**  
**DEPARTMENT OF MECHANICAL ENGINEERING**



**CERTIFICATE**

I hereby declare that the Project-I entitled " **EXPERIMENTAL INVESTIGATION ON TOOL VIBRATIONS DURING SURFACE DEFECT MILLING OF ZK60/ B<sub>4</sub>C / Al<sub>2</sub>O<sub>3</sub> HYBRID METAL MATRIX COMPOSITES**" submitted by the students **K. SAI RAM, K.KAMALAKAR, K. HEMANTH, M. DEVARAJ** is a record of original work carried out under my supervision during the academic year 2022-2023. The contents of this work, in full or in parts have not been submitted to any other institute or university for the award of any degree.

**Guide**

Dr B. RAVI SANKAR, Ph.D.  
Professor

**Head of the Department**

Dr . T. NANCHARAI AH, Ph.D.  
HOD & Professor

**Internal Examiner**

**External Examiner**

## ABSTRACT

The purpose of this research is to investigate on the influences of cutting parameters on machine tool vibration using Accelerometer in high precision milling machine. Magnesium is the most abundant metal. Its density level is 1.74–2.0 g/cm<sup>3</sup>, 33% lighter than aluminium and 77% lighter than steel. Magnesium alloy ZK60 based hybrid metal matrix composites were prepared with equal proportions of Al<sub>2</sub>O<sub>3</sub> and B<sub>4</sub>C reinforcements with varying weight fractions of 0%, 2%, 4%, 6% and 8%. The work piece is taken with the dimensions of 170mm length and 75 mm width and 45mm height. The present work investigated the influence of tool rotational speed, feed, depth of cut and weight fraction on torque. Carbide end mill with 12mm diameter, 75mm length and contains 4 flutes deployed for experimentation. Intentionally some grooves (SDM) are made on the surface with 0.2mm depth and 2mm width 75mm length for good machining. Tool vibrations are measured with the help of accelerometer. Tool rotational speed, feed, depth of cut and % of weight fraction are considered as input parameters in this investigation. Design of experiments techniques (DOE) has been employed to generate run order. End milling operation is performed by using Milling Machine. The results are to reveal that the effect of input parameters on induced vibrations (velocity, acceleration, and displacement). The Vibration acceleration amplitude is clearly influenced by the tool rotational speed and % weight fraction, and they are also strong significant values. The influence of feed rate & depth of cut on Vibration acceleration amplitude cannot be clearly demonstrated. The Vibration amplitude increases with an increase in spindle speed and % weight fraction. The Vibrations acceleration amplitude optimum at 250 rpm tool rotational speed, 10 mm/min feed, 0.75 mm depth of cut and 0% weight fraction.

**Keywords:** ZK60 Milling; Vibration; Accelerometer; Hybrid metal matrix composites; Surface defect machining (SDM); Design of experiments techniques (DOE); Milling Machine.

---

## ACKNOWLEDGEMENT

It is with immense pleasure that we would like to express our indebted gratitude to our guide **Dr B. RAVI SANKAR**, Ph.D., sir who has guided a lot and encouraged us in every step of thesis work.

We feel elated to thank our Head of the Department **Dr .T. NANCHARAI AH**, Ph. D inspiring us all the way and arranging all the facilities and resources needed for my thesis.

We also thank **Dr . NAZEER SHAIK**, Ph.D. Principal of Bapatla Engineering College, Bapatla, for providing excellent environment in the college.

We express our sincere thanks to all the teaching and non – teaching staff for providing the required impetus to complete thesis work.

KORAMUTLA SAI RAM	[L20AME502]
KOMMANAMANCHI KAMALAKAR	[L20AME498]
KHANDAVALLI HEMANTH	[L20AME496]
MARUPU DEVARAJ	[L20AME516]

## **CONTENTS**

<b>CHAPTER 1</b>	<b>INTRODUCTION</b>	<b>PAGE NO</b>
1.1	METAL MATRIX COMPOSITES (MMCs)	1
1.2	MANUFACTURING AND FORMING METHODS	2
1.3	MATRIX	6
1.4	REINFORCEMENTS	8
1.5	SURFACE DEFECTS MACHINING	12
1.6	MILLING	13
1.7	VIBRATIONS INDUCED DURING MILLING OPERATION	14
<b>CHAPTER 2</b>	<b>LITERATURE REVIEW</b>	<b>16</b>
2.1	NOTE	21
<b>CHAPTER 3</b>	<b>EXPERIMENTAL SETUP</b>	<b>22</b>
3.1	CASTING	24
3.2	HOLES FOR SETTING VIBROMETER	29
3.3	SDM(SURFACE DEFECT MACHINING)	31
3.4	EXPERIMENTATION	32
<b>CHAPTER 4</b>	<b>RESULTS AND DISCUSSION</b>	<b>37</b>
4.1	VIBRATIONS IN TOOL AXIS DIRECTION (Z-AXIS ACCELERATION AMPLITUDE IN M/S <sup>2</sup> )	39
4.2	VIBRATIONS IN TOOL MOVEMENT DIRECTION (X-AXIS ACCELERATION AMPLITUDE IN M/S <sup>2</sup> )	45
<b>CHAPTER 5</b>	<b>CONCLUSIONS</b>	<b>50</b>
5.1	VIBRATIONS IN TOOL AXIS DIRECTION (Z-AXIS ACCELERATION AMPLITUDE IN M/S <sup>2</sup> )	50
5.2	VIBRATIONS IN TOOL MOVEMENT DIRECTION (X-AXIS ACCELERATION AMPLITUDE IN M/S <sup>2</sup> )	50
<b>REFERENCES</b>		<b>51</b>

## LIST OF FIGURES

Figure No	Title	Page No.
1.1	Types of Metal matrix composite	1
1.2	Particles reinforced.	2
1.3	Stir casting line diagram.	4
1.4	Process of stir casting.	4
1.5	List of matrixes and reinforcements.	5
1.6	Types of magnesium alloys	6
1.7	ASTM designation system of magnesium	7
1.8	Types of reinforcements	8
1.9	Wettability of reinforcements	9
1.10	Selected reinforcement.	10
1.11	Use of patterning tool to make surface defects.	12
1.12	Schematic illustration of the two types of surface defect (grooves).	12
1.13	Conventional vs SDM work piece milling.	13
1.14	Milling Principle	13
1.15	Accelerometer Place on Work Piece (3d Image)	13
1.16	Vibration in different directions	15
1.17	Vibration acquisition	15
3.1	ZK60	22
3.2	B <sub>4</sub> C material	23
3.3	Al <sub>2</sub> O <sub>3</sub> material	23
3.4	Mechanical stirrer	24
3.5	Actual process of Stir Casting	25
3.6	Work Piece 3d Model.	29
3.7	Planning for holes	29
3.8	Bosch Professional Twist Drill for making holes.	30
3.9	Workpiece after making holes.	30
3.10	Planning for SDM	31
3.11	3-Axis CNC Milling Machine operated by SINUMERIK (808d,828d,840d)	31
3.12	Workpiece after SDM	32
3.13	3-AXIS Milling machine.	34
3.14	Carbide 4 Flutes End Mills 12mm Diameter 75mm Length (CNC Milling Cutter)	35
3.15	Vibrometer	36
3.16	Example Vibration Acceleration Signal Waveform in The Time Domain	37
4.1	Normal probability plot (Z-axis Acceleration Amplitude)	39
4.2	Main Effect Plot (Z-axis Acceleration Amplitude)	42
4.3	Interaction Plot (Z-axis Acceleration Amplitude)	42
4.4	Normal probability plot (X-axis Acceleration Amplitude)	45
4.5	Main Effects Plot (X-axis Acceleration Amplitude)	48
4.6	Interaction Plot (X-axis Acceleration Amplitude)	48

## LIST OF TABLES

Table No	Title	Page No
1.1	ZK60 properties	8
1.2	B <sub>4</sub> C & Al <sub>2</sub> O <sub>3</sub> properties	11
2.1	Literature	16
2.2	Literature	16
2.3	Literature	17
2.4	Literature	17
2.5	Literature	18
2.6	Literature	18
2.7	Literature	19
2.8	Literature	19
2.9	Literature	20
2.10	Literature	20
3.1	Masses of matrix and reinforcements	23
3.2	Weight fractions of work pieces.	24
3.3	Theoretical Calculations of work pieces volumes	26
3.4	Theoretical calculations of volume fractions	27
3.5	Composite density	28
3.6	Masses of matrix and reinforcements	28
3.7	Input variables	33
3.8	Total 31 experiment	33
3.9	3 axis Milling machine operated by siemens SINUMERIK 808d software.	34
4.1	Results From Experimentation	37
4.2	Analysis of Variance (Z-axis Acceleration Amplitude)	39
4.3	Model Summary (Z-axis Acceleration Amplitude)	40
4.4	Coefficients (Z-axis Acceleration Amplitude)	41
4.5	Analysis of Variance (X-axis Acceleration Amplitude)	45
4.6	Model Summary (X-axis Acceleration Amplitude)	46
4.7	Coefficients (X-axis Acceleration Amplitude)	47

# 1. INTRODUCTION

## 1.1 METAL MATRIX COMPOSITES (MMCs)

A metal matrix composite (MMC) is composite material with at least two constituent parts, one being a metal, The other material may be a different metal or another material, such as a ceramic or organic compound.

When at least three materials are present, it is called a **hybrid composite**.

### History

- Initial work in the late **1960s** was stimulated by the high-performance needs of the aerospace industry.
- **Steel-wire reinforced copper** were among the first continuous-fibre reinforced metal composites.
- **Boron filament** was the first high-strength, high modulus reinforcement in MMC.

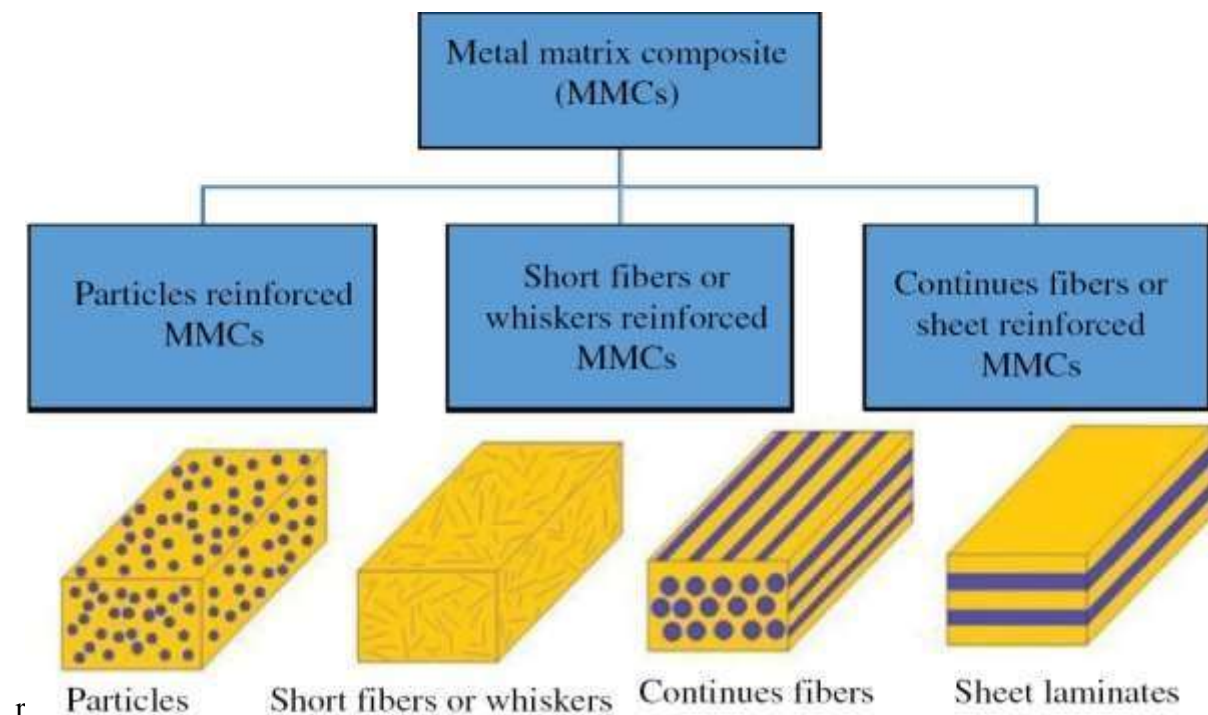


Fig.1.1 Types of Metal matrix composite



NOTE: **PARTICLES REINFORCED MMCs**

- Less Extensive than fibrous reinforcements
- Isotropic properties
- improves the machinability of the material.
- Compatible with most metal working process and often fabricated to near net shapes.
- increase the modulus of the matrix.
- Decrease the permeability of the matrix.
- Decrease the ductility of the matrix.
- Support higher tensile, compressive and shear stresses.
- Ability to tailor the mechanical properties through selection of reinforcement type and volume fraction along with the metal alloy.

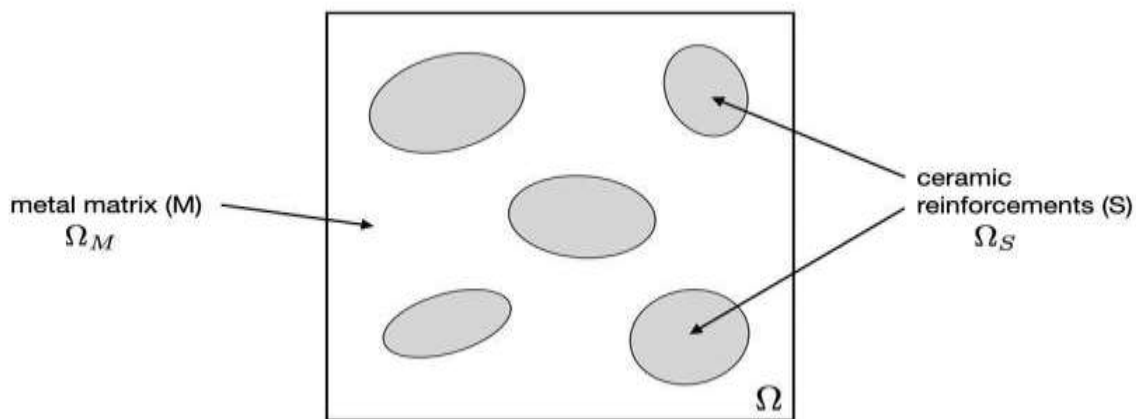


Fig.1.2 Particles reinforced

## 1.2 MANUFACTURING AND FORMING METHODS

- ★ Solid state methods
- ★ Semi-solid-state methods
- ★ Liquid state methods
- ★ Vapor Deposition
- ★ In-situ fabrication technique

NOTE: **LIQUID STATE METHODS**

Reference Article: Advanced liquid state processing techniques for ex-situ discontinuous particle reinforced nanocomposites: A review DOI: 10.1016/j.stmat.2018.05.005

C. Kannan, R. Ramanujan, School of Mechanical Engineering, VIT University, Vellore 632 014, India.

One advantage of the liquid state is the ease of forming because of the low viscosity. Complicated shapes can therefore be made with relative ease and at a low cost. Furthermore, it is relatively easy to mix materials in the liquid state to produce materials with specifically tailored composition.

### **Liquid state methods**

Liquid phase processing techniques can be classified into the following categories:

- (i) Sand casting
- (ii) Die casting.
- (iii) Squeeze casting
- (iv) Semisolid metal (SSM) casting
- (v) Stir casting.
- (vi) Spray forming
- (vii) Melt infiltration method.
- (viii) In situ synthesis

#### **NOTE: STIR CASTING**

Reference Article: Development of Magnesium Composite Material by the method of Stir Casting for applications in Automotive and Aerospace Industries.

The most cost-effective and simplest method of liquid state fabrication is stir casting. In this work stir casting technique is employed to fabricate the casted ingots. The reinforcement particles are in dispersed phase and is mixed with a molten metal by means of stirring for a particular period.

#### **STIR CASTING**

##### **➤ Stir casting process**

Stir casting is a type of casting process in which a mechanical stirrer is introduced to form vortex to mix reinforcement in the matrix material.

- It consists of
- A furnace
- Mechanical stirrer
- Crucible
- An electric motor
- Reinforcement feeder

The important parameters are **stirring speed, stirrer temperature, stirring time.**

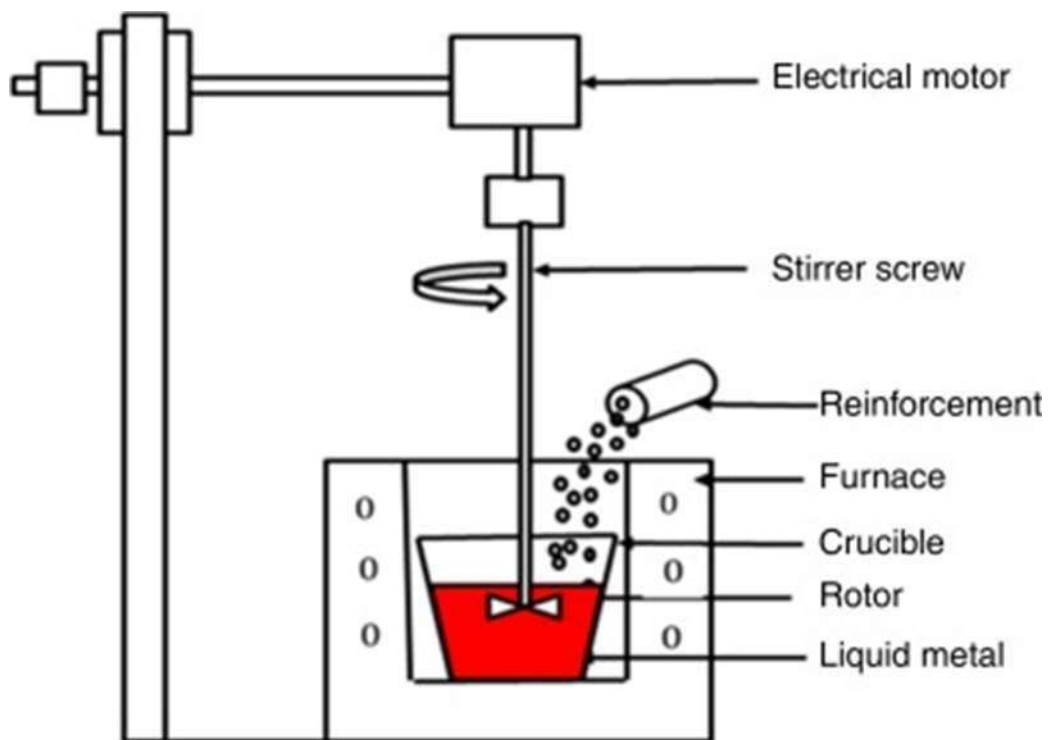


Fig.1.3 Stir casting line diagram

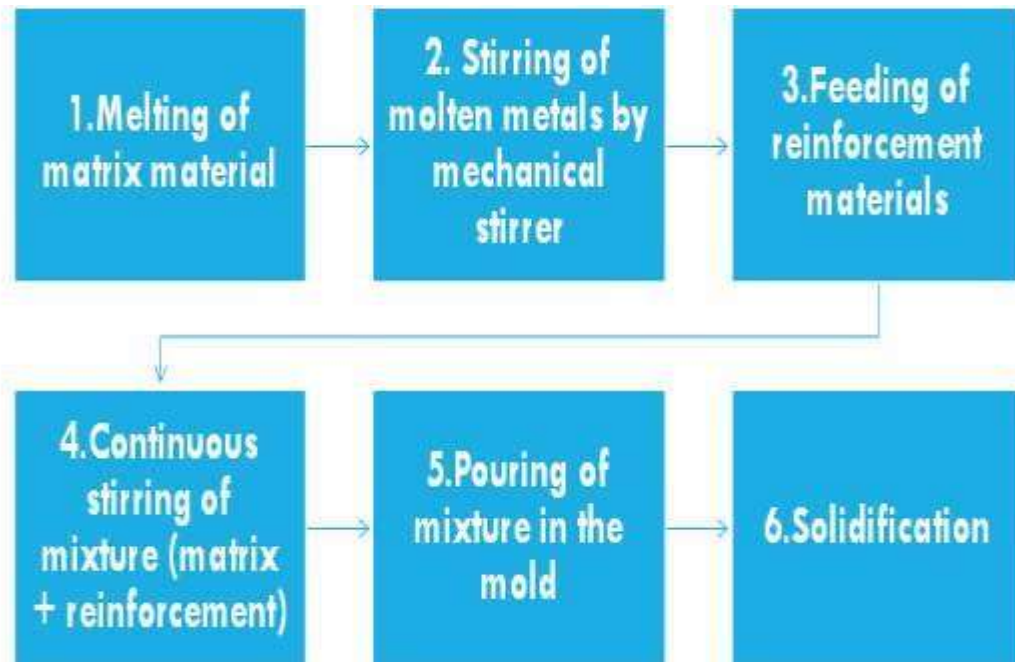


Fig.1.4 Process of stir casting

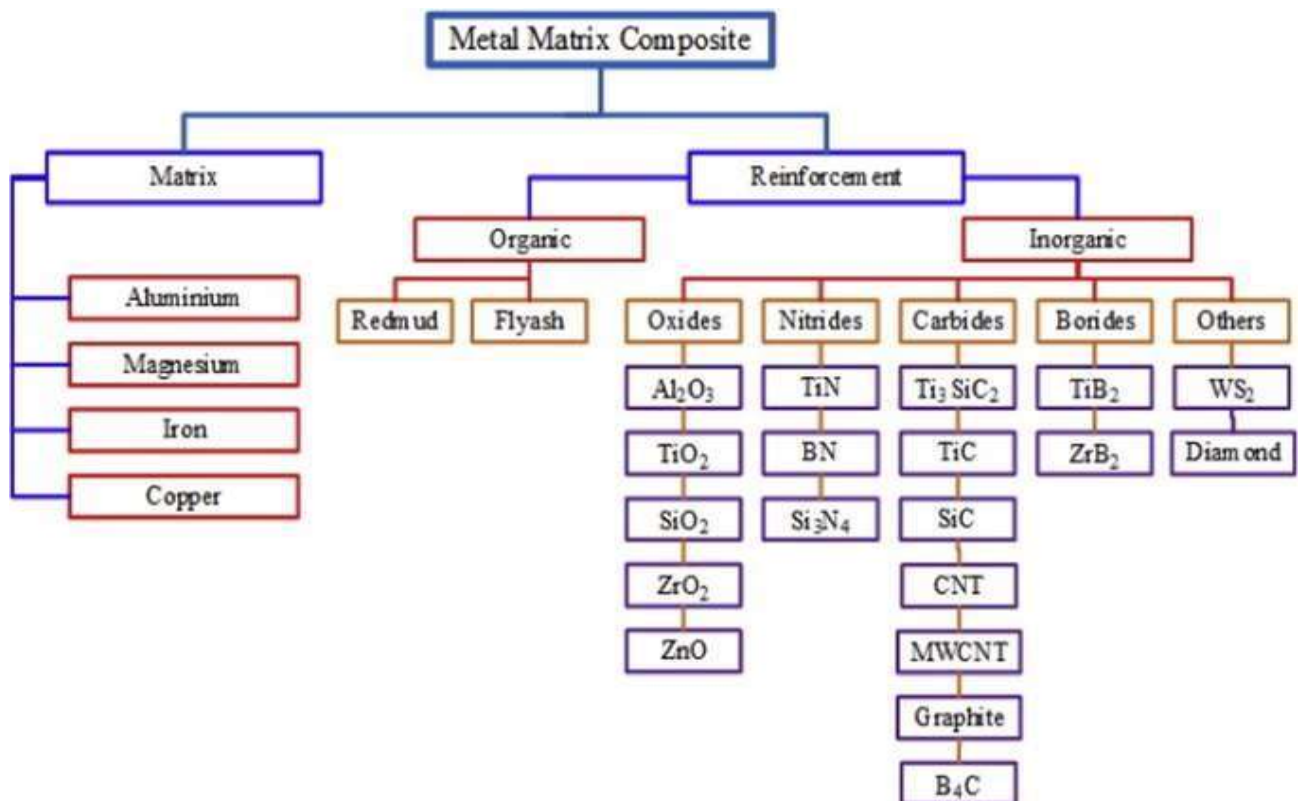


Fig.1.5 List of matrixes and reinforcements

### 1.3 MATRIX

Metal Matrix Composite (MMC) is a composite material with fibres or particles dispersed in a metallic matrix, such as copper, aluminium, or steel.

### APPLICATIONS

1. Automotive
2. Aerospace
3. Medical
4. Sports
5. Electronic
6. Other Applications

Magnesium is the lightest of all structural metals. It has a density of  $1.74 \text{ g/cm}^3$ , which is approximately one-fourth the density of steel and two-thirds that of aluminium. Because of its low density and high specific mechanical properties.

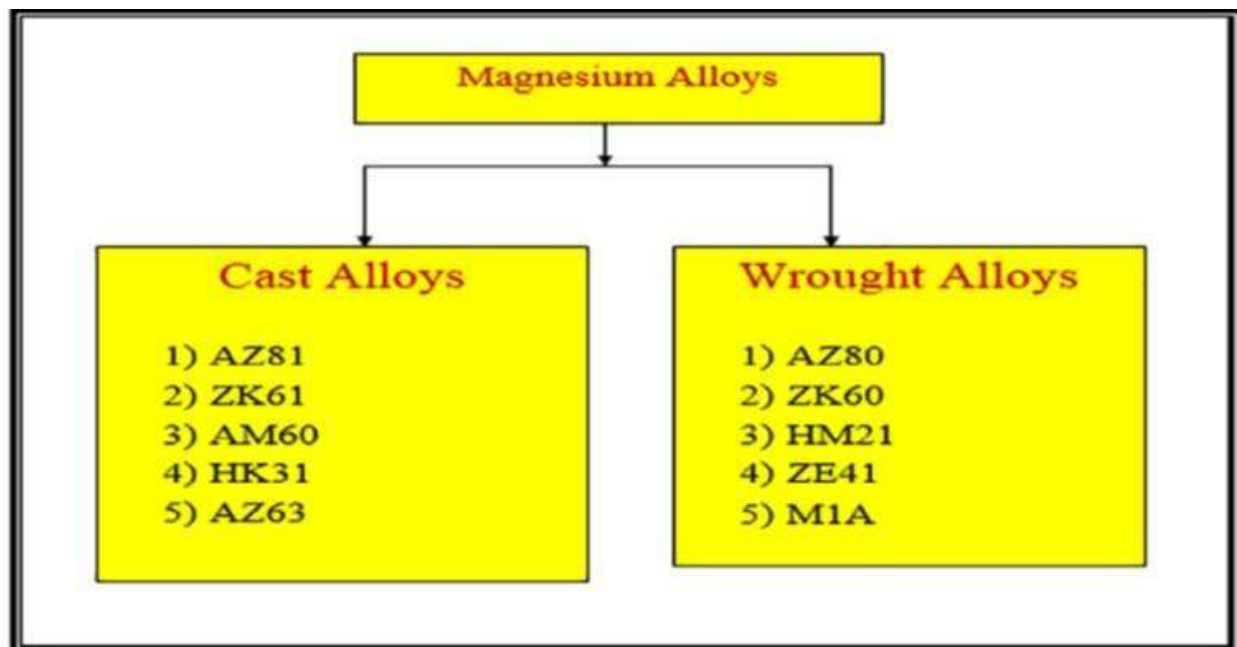


Fig.1.6 Types of magnesium alloys

**ASTM designation system of magnesium alloys [1, 16].**

Alloying element	Abbreviation letter
Aluminum	A
Bismuth	B
Copper	C
Cadmium	D
Rare earth metals	E
Iron	F
Thorium	H
Zirconium	K
Lithium	L
Manganese	M
Nickel	N
Lead	P
Silver	Q
Chromium	R
Silicon	S
Tin	T
Yttrium	W
Antimony	Y
Zinc	Z

**Fig.1.7 ASTM designation system of magnesium**

- A** First compositions, registered with ASTM
- B** Second compositions, registered with ASTM
- C** Third compositions, registered with ASTM
- D** High purity, registered with ASTM
- E** High corrosion resistance, registered with ASTM
- X** Experimental alloy, not registered with ASTM

For example, considering magnesium alloy AZ91C:

- AZ** Indicates that aluminum and zinc are the two main alloying elements
- 91** Indicates the percentages of aluminum and zinc (9 and 1, respectively), which are rounded-off to whole numbers
- C** Indicates the third specific composition registered having this nominal composition

**In magnesium matrix ZK60 having high mechanical properties, and few numbers of works had done on ZK60.**

## ZK60 properties (melting point 650°C)

Table 1.1 ZK60 properties

Properties	Metric
Tensile strength	365 MPa
Yield strength	305 MPa
Compressive yield strength	250 MPa
Shear strength	180 MPa
Shear modulus	17 GPa
Poisson's ratio	0.35
Hardness, Brinell (500 kg load, 10 mm ball)	88
Machinability (relative rating, 100=best)	100

## 1.4 REINFORCEMENTS

The synthesis of composite materials, reinforcements are intentionally introduced into the magnesium matrix. The reinforcements of different types, shapes, amounts, and length scales (micrometre size, sub-micrometre size, and nanosized), are judiciously selected to enhance the end properties of the base magnesium material to serve a specific application.

Type of Reinforcement	Name of Reinforcement	Symbol
Ceramic	Boron carbide	B <sub>4</sub> C
	Silicon carbide	SiC
	Titanium carbide	TiC
	Alumina, Aluminum oxide	Al <sub>2</sub> O <sub>3</sub>
	Magnesium oxide	MgO
	Tin oxide	SnO <sub>2</sub>
	Ytria, Yttrium oxide	Y <sub>2</sub> O <sub>3</sub>
	Zirconia, Zirconium oxide	ZrO <sub>2</sub>
	Titanium boride	TiB <sub>2</sub>
	Zirconium boride	ZrB <sub>2</sub>
Metallic	Aluminum	Al
	Copper	Cu
	Molybdenum	Mo
	Nickel	Ni
	Titanium	Ti
Others	Carbon	C
	Carbon nanotubes	CNTs

Fig.1.8 Types of reinforcements

To enhance the bond strength of the interface, it is essential that.

- (i) wetting between the matrix material and the reinforcement is promoted,
- (ii) the formation of oxide is minimized, and (iii) chemical interactions are controlled.

The two types of interfacial bonding between the reinforcement and the matrix in a metal matrix composite can be broadly grouped into ( I ) mechanical bonding (interlocking) and (ii) chemical bonding.

### Wettability

the wettability of a solid by a liquid is determined by the angle of contact which the liquid makes on the solid as shown. This contact angle ( $\theta$ ) is defined from the following young's equation.

Contact angle ( $\theta$ ) formed between the liquid, solid, and gas phases.



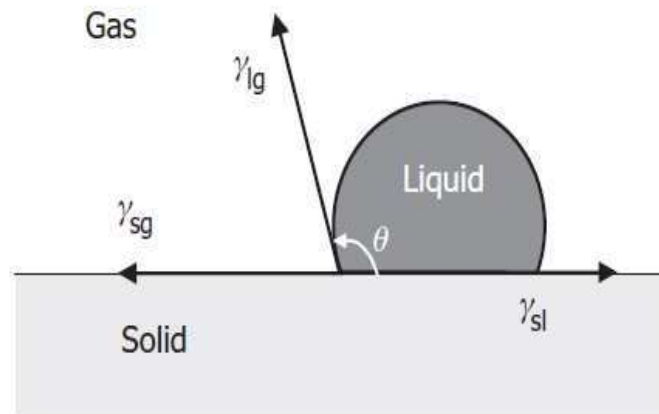


Fig.1.9 Wettability of reinforcements



$B_4C$



$Al_2O_3$

Fig.1.10 Selected reinforcement

### From the references

#### B<sub>4</sub>C

\*On the other side, it was shown that by enhancing the B<sub>4</sub>C content the macro-clusters of particles were not detected.

\* By increasing the B<sub>4</sub>C content, the wear behaviour of the composites was improved.

#### Al<sub>2</sub>O<sub>3</sub>

\*At lower strain rates, lattice self-diffusion is restricted by the presence of nano-alumina particles at the prior particle boundaries since the apparent activation energy is much higher than that for hot deformation of the matrix material which itself is close to that for lattice self-diffusion.

Table 1.2 B<sub>4</sub>C & Al<sub>2</sub>O<sub>3</sub> properties

B <sub>4</sub> C properties				Al <sub>2</sub> O <sub>3</sub> properties			
Property	Minimum Value (S.I.)	Maximum Value (S.I.)	Units (S.I.)	Property	Minimum Value (S.I.)	Maximum Value (S.I.)	Units (S.I.)
Density	3	3.98	g/cm <sup>3</sup>	Density	2.3	2.55	g/cm <sup>3</sup>
Melting Point	2277	2369	K	Melting Point	2645	2780	K

### Aluminium Oxide [Al<sub>2</sub>O<sub>3</sub>]

- Excellent mechanical, chemical and thermal properties.
- Good creep resistance.
- Compressive strength.

### Boron Carbide [B<sub>4</sub>C]

- Hardest element.
- High bonding strength.
- Flexural strength of hybrid composite
- it was shown that by enhancing the B<sub>4</sub>C content the macro-clusters of particles were not detected.
- the wear behaviour of the composites was improved.

### 1.5 SURFACE DEFECTS MACHINING

SDM is defined as a process of machining, where a workpiece is first subjected to surface defects creation at a depth less than the uncut chip thickness; either through mechanical and/or thermal means; then followed by a normal machining operation to reduce the cutting resistance.

\*Reduced cutting forces

\*Provide better surface finish and

\*Tool longevity

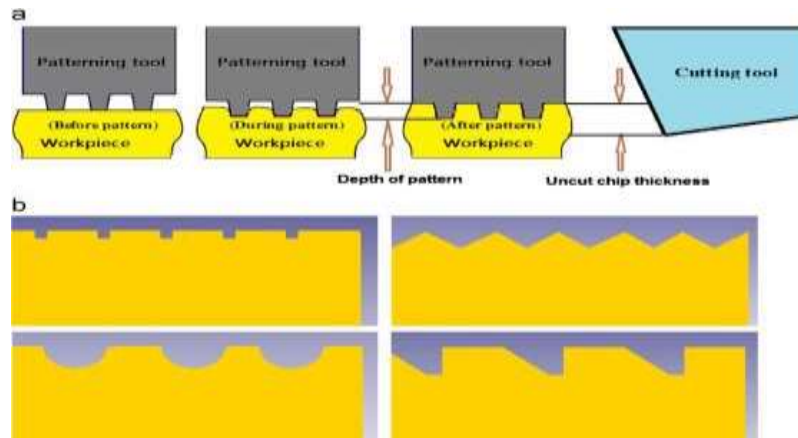
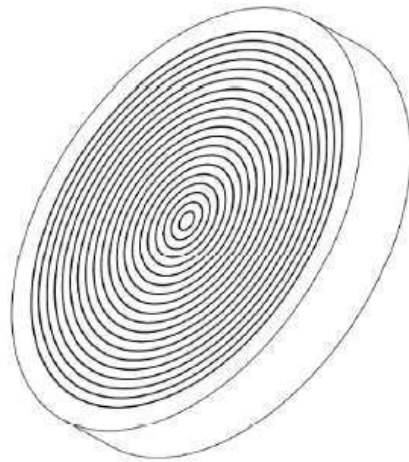
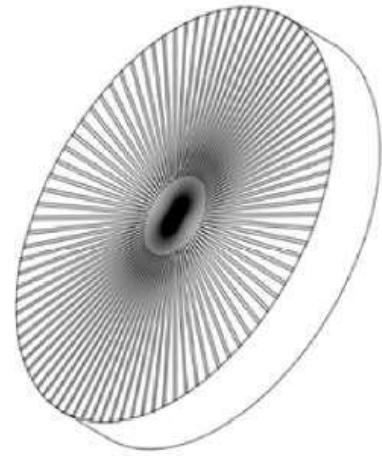


Figure -1.11 Use of patterning tool to make surface defects



(a) Grooves made in the circumferential direction



(b) Grooves made in the radial direction

Fig.1.12 Schematic illustration of the two types of surface defect (grooves)

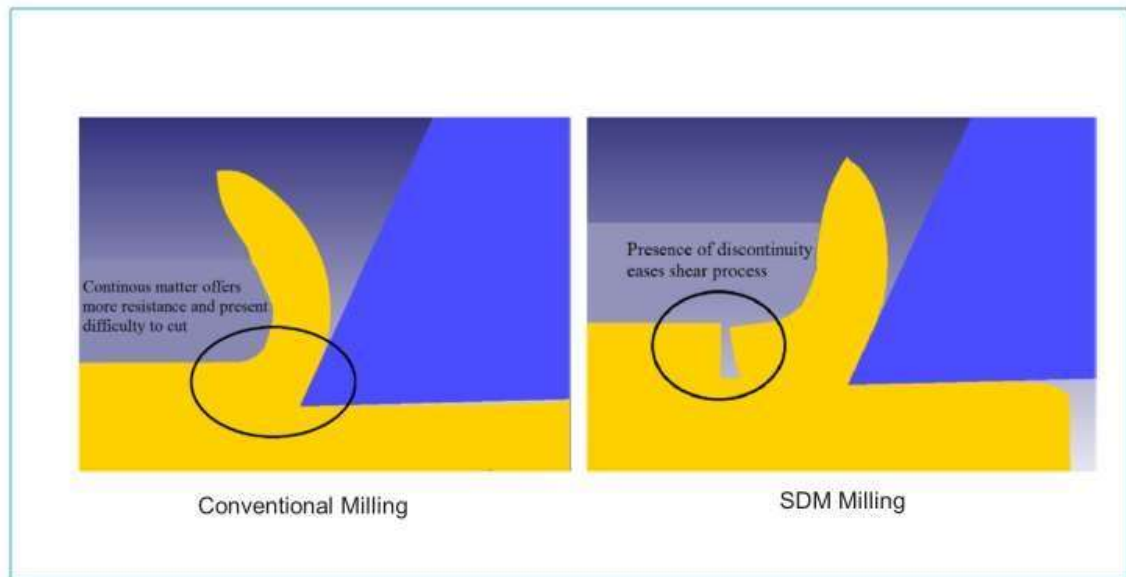
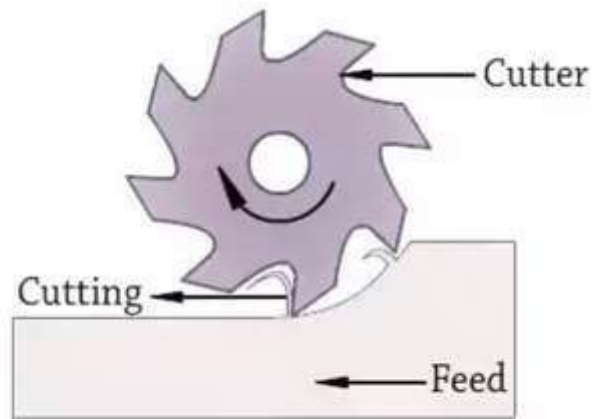


Fig.1.13 Conventional vs SDM work piece milling.

## 1.6 MILLING

In the milling process, metal is removed by moving the workpiece against a rotating multipoint milling cutter.



## Milling principle

Fig.1.14 Milling Principle

### 1.7 VIBRATIONS INDUCED DURING MILLING OPERATION

- Vibration is a by-product of the rotating tools common in milling. But excessive vibration leads to chatter, which causes wear on tools and machines—and worse can result in poor quality parts and excessive cycle times.

#### Chatter vibration

- Chatter is a form of cutting vibration that is caused by the characteristics of a machining system under the continuous action of aperiodic external exciting force. It usually shows the strong relative vibration between a tool and a workpiece in a metal cutting process.

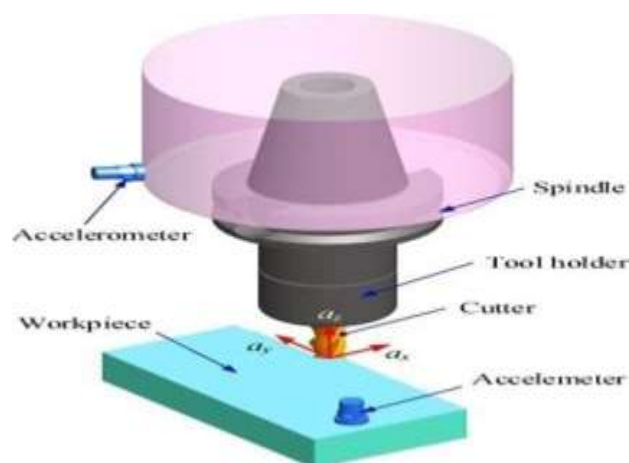


Fig.1.15 Accelerometer Place On Work Piece (3d Image)

#### The effect of vibration on the work piece

- The major effect is poor surface finish.
- Dimensional accuracy of job is also affected.

- This is mostly due to chatter vibration.
- Chatter marks are proof for the effect of vibration on the work piece **The effect of**

#### **vibration on the cutting condition**

- Three effects on cutting condition.
- Chip thickness variation effect
- Penetration rate variation effect
- Cutting speed variation effect

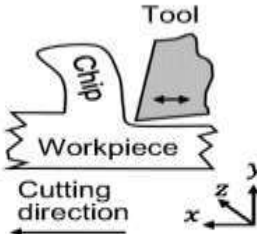
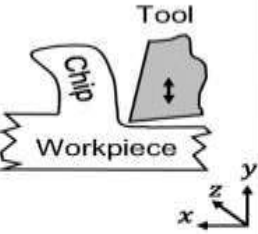
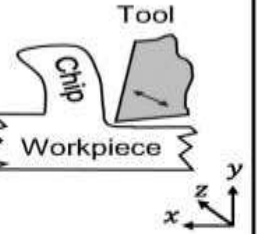

Type	Vibration in cutting direction	Vibration normal to the surface	Vibration normal to cutting direction	Combined vibration
Trajectory				
Displacement	$x(t) = v_c t + A_x \cos(2\pi f t)$ $y(t) = 0$ $z(t) = 0$	$x(t) = v_c t$ $y(t) = A_y \sin(2\pi f t)$ $z(t) = 0$	$x(t) = v_c t$ $y(t) = 0$ $z(t) = A_z \sin(2\pi f t)$	$x(t) = v_c t + A_x \cos(2\pi f t)$ $y(t) = A_y \sin(2\pi f t + \phi_1)$ $z(t) = A_z \sin(2\pi f t + \phi_2)$

Fig.1.16 Vibration in different directions

#### **Accelerometer**

- It measures the vibration, or acceleration of motion of a structure.
- converts mechanical energy into electrical energy.
- Vibration in rotating machines is monitored by accelerometer.
- It can be attached to the workpiece and the values can be observed in the VAS.

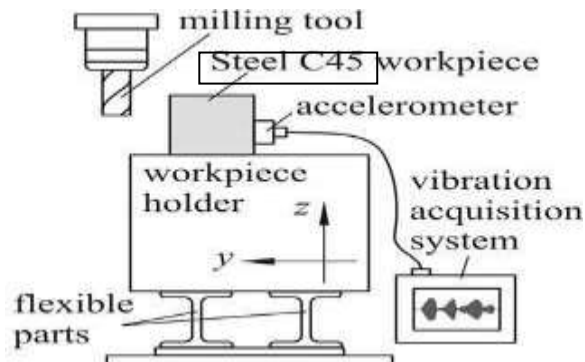
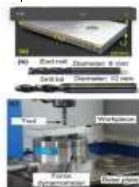
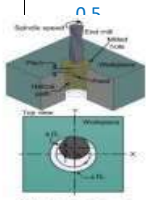


Fig.1.17 Vibration acquisition

## 2. LITERATURE REVIEW

Table 2.1

AUTHOR/Y EAR	MATRIX MATERIAL / DIMENSION S	TOOL MATERIAL & DIMENSIONS	INPUT PARAMETERS	RESPONSES /OUTPUTS MEASURED	CONCLUSION / REMARKS
<b>Experimental investigation on the performance of helical milling for hole processing in AZ31 magnesium alloy</b>					
Justin Aral Gonsalves, Sadvidya N. Nayak, Gururaj Bolar  2020	AZ31 Magnesium Alloy (110 X 50 X 12) mm <sup>3</sup>	two fluted solid carbide end mills having a helix angle of 35° helix, 12 mm diameter and 8 mm diameter	*Spindle speed (rev/min) 2000 4000 6000 *Feed per tooth (mm/z) 0.05 0.10 0.15 *Axial pitch (	*Surface roughness (mm) *Axial force (N)  *Radial force (N) *Machining temperature (C)	Spindle speed was found to be a highly influential parameter impacting the surface finish. The superior surface finish was noted when the machining was carried out at 6000 rev/min. Feed per tooth was found to influence surface finishing negatively with poor surface finish noted at a high feed value of 0.15 mm/z. Analysis of machining temperature showed that spindle speed was the most influential parameter with temperature increasing with spindle speed. The shape and size of the chips varied with the feed per tooth and axial pitch. The shape of the chips changed from short conical helical to folded long ribbon type with the increase in feed per tooth and axial pitch. Also, segmentation and breakability of chips increased with the increase in feed value. Chip segmentation and breakage were noted at higher feed values. The thickness of the lamellar structure on the chip increased with the increase in chip size.



AUTHOR / YEAR	MATRIX MATERIAL / DIMENSION S	TOOL MATERIAL & DIMENSIONS	INPUT PARAMETERS	RESPONSES /OUTPUTS MEASURED	CONCLUSION / REMARKS
<b>Effect of cutting parameters on machinability characteristics in milling of magnesium alloy with carbide tool</b>					
Kaining Shi, Dinghua Zhang, Junxun Ren, Changfeng Yao and Xinchun Huang  Date received: 3 June 2015; accepted: 10 December 2015  1. effect of cutting speed at feed rate of 0.8 mm/r, 2. effect of feed rate at cutting speed of 200 m/min	AZ91D  110 mm 3 65 mm 3 55 mm	Depth of cut( mm )1.5 Width of cut (mm) 3 Number of tooth – 1. Milling type – End-milling Coolant – Dry Tool material – Carbide	Cutting speed (V) m/min 50, 100, 200, 400 Feed rate (f) mm/r 0.4, 0.6, 0.8	surface roughness cutting force chip formation	*The cutting force decreases with the increasing cutting speed. And yet for a given cutting speed, cutting force increases with the rising of feed rate due to heavy chip load. In all cutting conditions, it is found that the feed force is higher than the radial force. *By considering the chip formation process, it can be concluded that the chip quality is affected by feed rate, while the chip morphology is driven by cutting speed. The chip back surface changes from fine saw-tooth to poor saw-tooth which is related to the increased feed rate. *Ideal surface finish is produced when either better chip morphology or small broken chip was formed during the milling process. Therefore, the chip quality or chip size could be used as an important criterion for evaluating the machined surface quality.

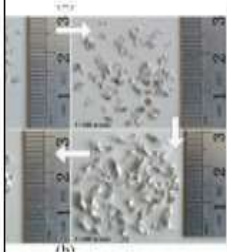


Table 2.2



Table 2.3

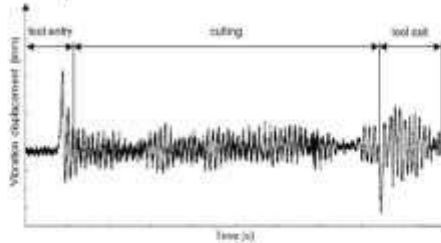
AUTHOR / YEAR	MATRIX MATERIAL / DIMENSIONS	TOOL MATERIAL & DIMENSIONS	INPUT PARAMETERS	RESPONSES /OUTPUTS MEASURED	CONCLUSION / REMARKS
<b>Effect of rare earth oxide on the properties of laser cladding layer and machining vibration suppressing in side milling</b>					
Yanhua Zhong, b. Jie Song, b. *, Jianfeng	Mg–6Zn–3Cu and ZK60 Alloys (Dimensions not given)	the diameters (D) of the tools are 20 mm with equal overhang length	<p><i>QFeed f (mm/tooth)</i> 0.02 0.04 0.08</p> <p><i>Axial Doc ap (mm)</i> 4 8 12 16</p> <p><i>Cutting speed V (m/min)</i> 150</p> <p><i>Radial Doc ae (mm)</i> 0.3</p>	<p>Hardness</p> <p>Wear Resistance *The impact of La2O3 on surface roughness</p> <p>Frequency domain analysis</p>	<p>The properties of the coatings and the milling vibration characteristics were investigated. The major conclusions can be summarized as follows:</p> <ul style="list-style-type: none"> <li>The hardness and wear resistance is improved significantly which may be due to the metal-strengthening by grain size reduction.</li> <li>Machining vibrations of LCL with La2O3 addition are significantly reduced and the chatter is effectively avoided occurring. This may be due to the damping capacity of LCL with La2O3 addition is enhanced.</li> </ul>
1 December 2014					 <p>Figure 1. The waveform of the vibration displacement signal presented as a function of time.</p>

Table 2.4

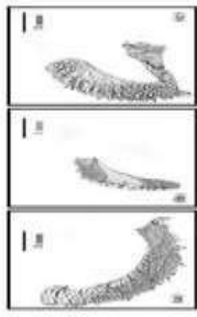
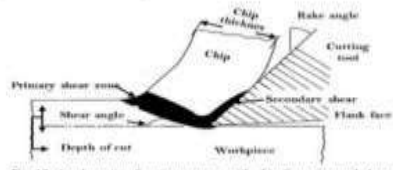
AUTHOR / YEAR	MATRIX MATERIAL / DIMENSIONS	TOOL MATERIAL & DIMENSIONS	INPUT PARAMETERS	RESPONSES /OUTPUTS MEASURED	CONCLUSION / REMARKS
<b>Application of Environmentally friendly Cooling/Lubrication Strategies for Turning Magnesium/SiC MMCs</b>					
Navneet Khanna1 & Prassan Shah1 & Narendra Mohan Suri2 & Chetan Agrawal1 & Sandeep K. Khatkar 3 & Francis Pusavec4 & Murat Sarikaya	AZ91/5SiC ( $\phi = 20$ mm, 190 mm length) fabricated using an in-house developed stir casting setup Silicon Carbide 67 g/cm <sup>3</sup>	Uncoated Kyocera made CNMG120404 AH PDL025 inserts Orthogonal rake angle = $-6^\circ$ inclination angle = $-6^\circ$ , clearance angle = $6^\circ$ Primary cutting-edge angle ( $\psi$ ) = $95^\circ$ nose radius ( $r_n$ ) = 0.4 mm, insert thickness = 4.76 mm, size of insert describing the diameter of inscribed circle = 12.7 mm	<p>Depth of cut (mm) 0.5</p> <p>Vc (m/min) 62, 41 and 27 f (mm/rev) 0.111, 0.222 and 0.333</p>  <p>Fig. 11. Segmented chip formation during turning of AZ91/5SiC MMCs</p>	<p>Chip type (Cryon MQL)</p> <ol style="list-style-type: none"> <li>1. Arc / Bulky</li> <li>2. Circular</li> <li>3. Ribbon</li> </ol>	<p>Segmented type of chips is found for all cooling and lubrication techniques. The comparable values of chip breakability index are observed for CryoMQL, cryogenic and MQL machining. However, higher value of <math>C_{in}</math> is found for LN2 as cutting fluid in comparison with MQL and CryoMQL machining at <math>vc1f3</math>.</p> <p>The 40.39% and 64.65%; 7.13% and 11.49% higher value of cutting force and energy consumption is found correspondingly for CryoMQL and cryogenic machining respectively in comparison with MQL technique by considering the mean of all turning tests. The 25.59% and 18.35% lower values of <math>R_a</math> have been observed in case of CryoMQL machining considering all turning tests, as compared to MQL and cryogenic machining respectively.</p> <p>The increment in hardness of workpiece material is responsible for generating higher cutting force and energy consumption in cryogenic and CryoMQL techniques. The lower values of <math>R_a</math> observed in MQL machining is due to adhesion of SiC particles on cutting tool.</p>  <p>Fig. 12. A schematic of cutting process with chip formation and shear zone indication [41]</p>



Table 2.5


AUTHOR / YEAR	MATRIX MATERIAL / DIMENSIONS	TOOL MATERIAL & DIMENSIONS	INPUT PARAMETERS	RESPONSES /OUTPUTS MEASURED	CONCLUSION / REMARKS
<b>Influence of Tool Holder Types on Vibration in Rough Milling of AZ91D Magnesium Alloy</b>					
Ireneusz Zagórski 1,*, Jarosław Korpysa 1 and Andrzej Weremczuk 2 Received: 14 April 2021 Accepted: 11 May 2021 Published: 12 May 2021	AZ91D Magnesium Alloy 112 mm × 150 mm × 56 mm	Three types of tool holders with a HSKA63 spindle were used for tool clamping: ER 32 × 100 SECO collet chuck (Fagersta, Sweden), SFD 16 × 120 SECO heat shrink chuck (Fagersta, Sweden), and Tendo E compact 20 × 80 Schunk hydraulic chuck (Lauffen/Neckar, Germany) (power 25 kW, nmax up to 24,000 rpm, and v <sub>f</sub> max up to 40 m/min). TiAlN coating, recommended for aluminium and magnesium milling applications. It was a 2-flute tool, diameter d = 36 mm, overall dimensions 16 × 25 × 100 mm <sup>3</sup> , and helix angle λs = 30°. The milling process was performed as downmilling, along with straight toolpaths.	Cutting speed v <sub>c</sub> (m/min) 400 600 800 1000 Feed per tooth f <sub>z</sub> (mm/tooth) 0.05 0.10 0.15 0.20 0.25 0.30	maximum vibration acceleration values rms vibration acceleration value	<ul style="list-style-type: none"> <li>the selection of an appropriate configuration of technological parameters enabled a significant improvement in the stability of the magnesium alloy milling process;</li> <li>increasing the cutting speed and feed per tooth caused an increase in all values characterising the vibration displacement, except for v<sub>c</sub> = 1000 m/min for which a decrease in the value was observed;</li> <li>the type of tool holder did not have a clear impact on the obtained values describing the vibration displacement;</li> <li>increasing the cutting speed and feed per tooth increased all the values describing the acceleration of vibrations;</li> <li>several times lower values characterising the vibration acceleration, by changing either the cutting speed or the feed per tooth,</li> </ul> 

Table 2.6

AUTHOR /YEAR	MATRIX MATERIAL / DIMENSIONS	TOOL MATERIAL & DIMENSIONS	INPUT PARAMETERS	RESPONSES /OUTPUTS MEASURED	CONCLUSION / REMARKS
<b>A Consideration of Tool Wear Mechanism when Machining Metal Matrix Composites (MMC)</b>					
K. Weinert, ISF, University of Dortmund/ Germany - Sponsored by W. König (I), RWTH Aachen/Germany Received on January 11, 1993	The machining of 6-Al10, and SiC reinforced aluminium	Solid bodies are the different cutting materials cemented carbides and polycrystalline diamonds with different grain, which have been used	Cutting material cemented carbide (medium grain) Cutting speed v <sub>c</sub> = 100 m/min Depth of cut a <sub>p</sub> = 1 mm Feed rate: t = 0.1 mm/rev	Tool wear of cemented carbide when turning reinforced aluminium; SEM photographs of cemented carbides used for cutting reinforced aluminium Tool wear when machining reinforced aluminium with different cemented carbides Tool wear when machining reinforced aluminium with PCD	For the machining of 6-Al10, reinforced aluminium the wear resistance of fine-grained cemented carbide is improved against the standard medium grain size. The reason for this result is the higher toughness of the fine-grained cemented carbide, by which the resistance against microcracking and fatigue can be improved. In the case of SiC or BE reinforced aluminium the increase of the grain size of cemented carbide on the flank wear rate is reversed. The main wear mechanism is abrasion by micro cutting. Therefore, the wear rate can be derived by using coarse grained cemented carbide. The wear mechanism is corresponding to the mechanism when cutting SiC and B <sub>4</sub> C Reinforced aluminium with cemented carbide. The wear resistance of PCD 025 is improved compared to PCD 010 cause the grains are larger than the reinforcement particles of the composites. Therefore PCD 025 better withstands an abrasion wear by micro cutting. This argumentation is supported by the results of the investigations about the wear mechanisms when machining unreinforced aluminium (AlSi12) with PCD. In this case the main wear mechanism is abrasion which produces grooves at the PCD tools. This is referred to the formation of alumina at the tool which could be hard enough to produce grooving wear at PCD

Table 2.7

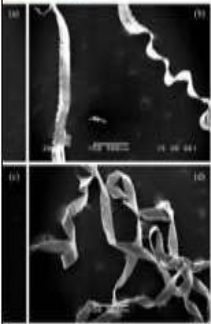
AUTHOR /YEAR	MATRIX MATERIAL / DIMENSIONS	TOOL MATERIAL & DIMENSIONS	INPUT PARAMETERS	RESPONSES /OUTPUTS MEASURED	CONCLUSION / REMARKS
<b>Effect of Cutting Parameters on Ignition of AM50A Mg Alloy during Face Milling</b>					
J. Z. Hou <sup>12</sup> , Wei Zhou <sup>13</sup> , and N. Zhao Published online: 13 Dec 2010.	AM50A magnesium alloy	CNC milling machine Mazak FJV-250. The rake angle of metal carbide indexable face milling is 34 and radius of clean-up is 40 mm. The width of cut is 55 mm, which is equal to the width of workpiece.  The morphology of chip under different ignition conditions 	Cutting speed (rpm) 1000, 2000, 3000, 4000, 5000, 6000, Feed rate : 200 mm/min, 400 mm/min, 600 mm/min, 800 mm/min, 1000 mm/min, Depth of cut 1 $\mu$ m 4 $\mu$ m 80 $\mu$ m	Influence of cutting speed and feed rate on chip ignition Effect of Chip Morphology	It is interesting to find that ignition occurs when the milling parameters are in the moderate range. We found that ring of fire could be easily produced by intertwined chips (100 mm/min $\leq$ feed rate $\leq$ 400 mm/min, 2000 rpm $\leq$ cutting speed $\leq$ 4000 rpm, depth of cut = 4 m).

Table 2.8

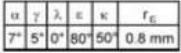
AUTHOR /YEAR	MATRIX MATERIAL / DIMENSIONS	TOOL MATERIAL & DIMENSIONS	INPUT PARAMETERS	RESPONSES /OUTPUTS MEASURED	CONCLUSION / REMARKS
<b>Machining of Magnesium Workpieces</b>					
By Thomas Eriemuth and Jens Winkler*	alloy used is AZ91 Workpieces were sand-cast bars of 150 mm in diameter	Uncoated carbide tools (HW) and tools with polycrystalline diamond (DP) tips, as well as TiN and diamond-coated carbide tools (HC TiN, HC DP), were used.	workpiece : AZ91 HP T6 cutting speed : $v_c = 900$ m/min feed : $f = 0.4$ mm depth of cut : $a_p = 1.5$ mm cooling lubricant : none  tool material : HW K10 geometry : CCMT 120408 	Tool wear when machining a magnesium based MMC,  Influence of the rolling force on workpiece properties.	DP cutting tools show a superior behaviour in dry machining magnesium alloys compared to uncoated and TiN-coated cemented carbide tools. Adhesion between cutting tool and workpiece material, as well as material build-up, can best be avoided if diamond coatings are used. Because machining forces are low when using DP tools, the chip temperature and therefore the danger of chip ignition can be reduced. When machining magnesium-based MMC, DP-tipped tools are preferred because they have the best resistance against abrasion. Burnishing operations are a useful mean of improving surface quality and hardness, and of inducing compressive stresses in the subsurface. Rolling forces above $F_r = 3$ kN may lead to damage in the surface of the used AZ91. The rolling in of a ceramic reinforcement can be applied to increase the wear resistance. Good results were found for SiC particles of relative coarse grain.



Table 2.9

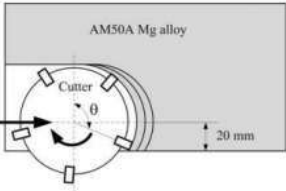
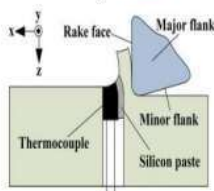
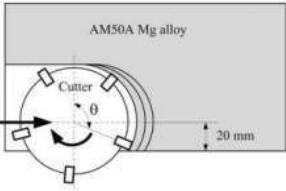
AUTHOR /YEAR	MATRIX MATERIAL / DIMENSIONS	TOOL MATERIAL & DIMENSIONS	INPUT PARAMETERS	RESPONSES /OUTPUTS MEASURED	CONCLUSION / REMARKS
<b>Influence of Cutting Speed on Flank Temperature during Face Milling of Magnesium Alloy</b>					
Junzhan Hou , Ning Zhao & Shaoli Zhu  Accepted author version posted online: 27 May 2011. Published online: 08 Apr 2011.	AM50A commercial magnesium alloy  Dimensions of the workpiece were 150 mm × 100 mm × 21 mm.	CNC milling machine (Mazak FJV-250).  The diameter of indexable face milling cutter was 80 mm.  Tool insert was K110M of kennametal carbide	<b>spindle speed:</b> 600 rpm, 1000 rpm, 2000 rpm, 4000 rpm, 6000 rpm, 8000 rpm, 10000 rpm, and 12000 rpm <b>Feeding speed</b> 60 mm/min, 100 mm/min, 200 mm/min, 400 mm/min, 600 mm/min, 800 mm/min, 1000 mm/min, and 1200 mm/min <b>Feed rate of 0.02 mm/tooth</b> was adopted in the experiment. <b>Cutting speed</b> 151 m/min–3014 m/min <b>Depth of cut</b> 15 mm <b>width of cut</b> 60 mm. Cooling and lubricating Dry	Mean Flank Temperature under Different Cutting Speed	The temperature rise increases slightly Downloaded by [UNAM Ciudad Universitaria] at 20:50 23 December 2014 <b>INFLUENCE OF CUTTING SPEED ON FLANK TEMPERATURE</b> 1063 when the cutting speed is less than 1507 m/min. It is interesting that the chip ignition can be observed under these conditions. It exists in the cutting zone when the mean flank temperature rise is near 3C only in the cutting process at ambient temperature. When the cutting speed is up to be more than 1507 m/min, the temperature rise increases significantly, but the chip ignition cannot be seen. By further increasing the cutting speed, the mean flank temperature rise falls down in case that the cutting speed is 3014 m/min.
					
FIGURE 3.—The milling process of magnesium alloy.		FIGURE 5.—The schematic diagram of temperature measurement in face milling (color figure available online).			

Table 2.10

AUTHOR /YEAR	MATRIX MATERIAL / DIMENSIONS	TOOL MATERIAL & DIMENSIONS	INPUT PARAMETERS	RESPONSES /OUTPUTS MEASURED	CONCLUSION / REMARKS
<b>High speed cutting of AZ31 magnesium alloy</b>					
Yixei Lu a,b, Shaobua Hu, Longfei Liu, Zhensu Yin  Received 2 April 2016; revised 20 April 2016; accepted 26 April 2016.	AZ31 magnesium alloy  cutting billets was $\Phi 23 \text{ mm} \times 200 \text{ mm}$	LBR-370 numerical control lathe, cutting tool 15 mm in length, 15 mm in width, 5 mm in thickness, cutting edge angle was $6^\circ$ , the cutting edge radius was 0.2 mm.	Speed (r/min) 1000 1400 1800 2200 Depth(mm) 0.5 1 1.5 2 Feed rate 0.02 0.05 0.08 0.11	Microstructure, Hardness, Roughness,	The stress layer depth decreases with the increase of the cutting speed. Hardness reduces from the edge to interior at each cutting condition. The variation range is within about $20 \mu\text{m}$ , Roughness reduces with the increase of cutting speed, while it increases with the increase of depth and feed rate. All the variation range is within about $1 \mu\text{m}$

## 2.1 Note

- 1.Vibration amplitude increases with an increase in spindle speed and cutting depth.
- 2.Overall, within the whole testing conditions, the influence of feed rate on machining vibration cannot be clearly demonstrated.

[ Reference ; Yung- Chih Lin et all]

- The vibration levels are closely related to the cutting parameters, and they increase with an increase in the cutting speed and feed rate.

[ Reference: Qadri, M.O et all, Bhuiyan, M.S.H et all, Kiew, C.L et all ]

- That cutting speed is a major factor affecting tool vibration, which thereby affects surface finish .

[ Reference: Bhogal et al]

- The type of tool holder did not have a clear impact on the obtained values describing the acceleration of vibrations.

[ Reference: Ireneusz et al] .....etc

### 3. EXPERIMENTAL SETUP

#### 3.1 Casting

This project addresses the detailed development stages of ZK60- $\text{Al}_2\text{O}_3$ -  $\text{B}_4\text{C}$  hybrid metal matrix composite (HMMC) through stir casting route. The composites were prepared using stir casting method in which amount of reinforcement is varied from 0-8% in steps of 2wt%. During stir casting process, the melting action of material emits out certain gases and residual apart from the required composite. The residuals have certain environmental concerns, which need to be addressed, since some of the gases and solid waste can cause adverse effects to the environment in terms of air and soil pollution. The severe affects have been addressed of such residuals on the environment.

workpiece is first subjected to surface defects creation at a depth less than the uncut chip thickness; either through mechanical and/or thermal means; then followed by a normal machining operation to reduce the cutting resistance.

Vibration isn't always avoidable and is often an indicator of the conditions and load being experienced by your machine. As such, it is important to monitor vibration because it can: Indicate wear that is compromising machining ability/reducing tool life. Impact finish and part accuracy.

#### Matrix

ZK60

(Melting Temperature: 650 °C)

ZK60A — Zn(5.5)+ Zr(0.7)+Mg(93.8)



Fig.3.1 ZK60

### Reinforcements

#### 1. $B_4C$

Melting Temperature: 2,350 °C

Grain size: 60 microns



**Fig.3.2  $B_4C$  material**

#### 2. $Al_2O_3$

Melting Temperature: 2,072 °C

Grain size: 40 microns



**Fig.3.3  $Al_2O_3$  material**

### **Mass Of Matrix & Reinforcements From Theoretical Calculations**

**Table 3.1 Masses of matrix and reinforcements**

<b>Work piece</b>	<b>mass MATRIX</b>	<b>R-1</b>	<b>R-2</b>
1	1154.95875	0	0
2	1141.108469	11.64	11.64
3	1141.108469	11.64	11.64
4	1127.02997	23.47	23.47
5	1127.02997	23.47	23.47
6	1112.717566	35.51	35.51
7	1112.717566	35.51	35.51
8	1098.165379	47.74	47.746

## Stir Casting

Stir casting is a type of casting process in which a mechanical stirrer is introduced to form vortex to mix reinforcement in the matrix material.



Work piece	weight fractions(%)		
	Matrix	Reinforcement-1	
1	100	0	0
2	98	1	1
3	98	1	1
4	96	2	2
5	96	2	2
6	94	3	3
7	94	3	3
8	92	4	4

Fig.3.4 Mechanical stirrer

Table 3.2 Weight fractions of work pieces.

## Process of Stir Casting

Stir casting is a type of casting process in which a mechanical stirrer is introduced to form vortex to mix reinforcement in the matrix material. It is a suitable process for production of metal matrix composites due to its cost effectiveness, applicability to mass production, simplicity, almost net shaping and easier control of composite structure.

The furnace is used to heating and melting of the materials. The bottom pouring furnace is more suitable for the stir casting as after stirring of the mixed slurry instant pouring is required to avoid the settling of the solid particles in the bottom of the crucible. The mechanical stirrer is used to form the vortex which leads the mixing of the reinforcement material which are introduced in the melt. Stirrers consist of the stirring rod and the impeller blade. The impeller blade may be of various geometry and various number of blades. Flat blade with three number is the preferred as it leads to axial flow pattern in the crucible with less power consumption. This stirrer is

connected to the variable speed motors, the rotation speed of the stirrer is controlled by the regulator attached with the motor. Further, the feeder is attached with the furnace and used to feed the reinforcement powder in the melt. A permanent mould, sand mould or a lost-wax mould can be used for pouring the mixed slurry. In this process, the matrix material is kept in the bottom pouring furnace for melting. Simultaneously, reinforcements are preheated in a different furnace at certain temperature to remove moisture, impurities etc. After melting the matrix material at certain temperature, the mechanical stirring is started to form vortex for certain time then reinforcements particles are poured by the feeder provided in the setup at constant feed rate at the centre of the vortex, the stirring process is continued for certain time period after complete feeding of reinforcements particles. The molten mixture is then poured in preheated mould and kept for natural cooling and solidification.

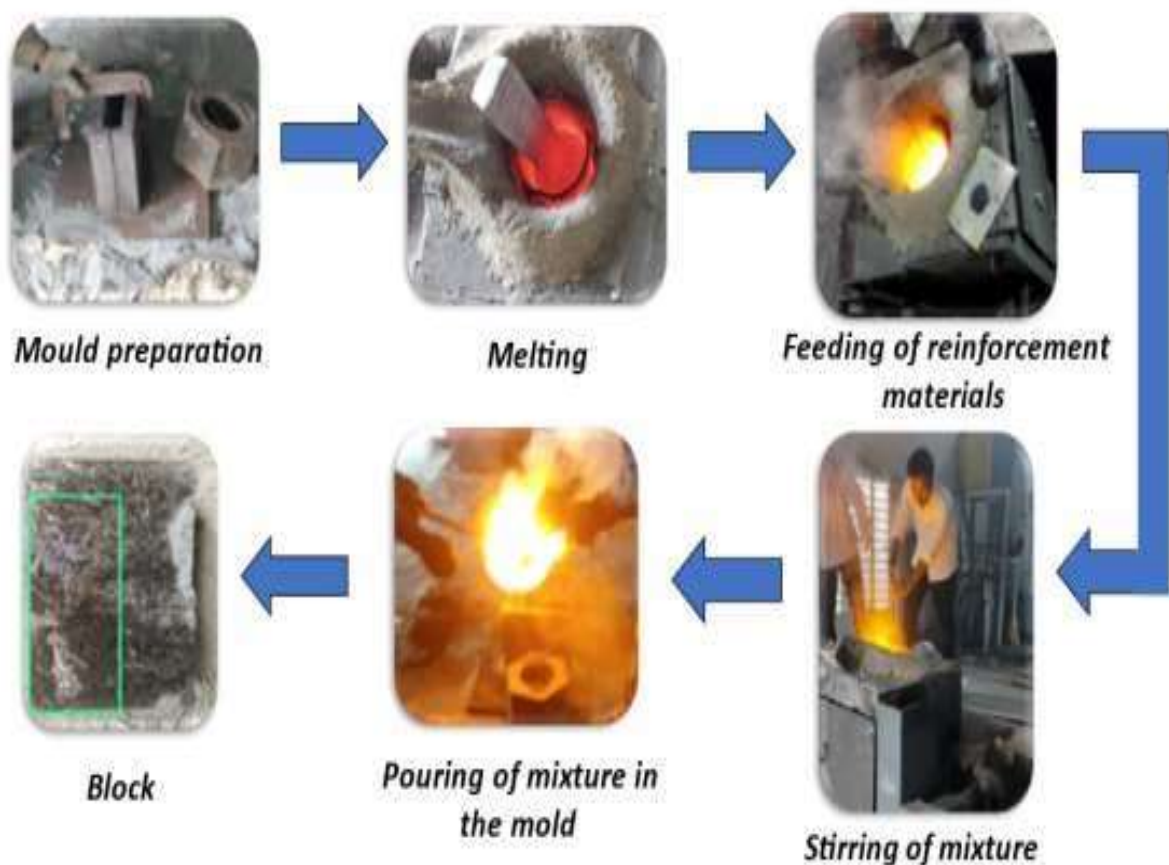


Fig.3.5 Actual process of Stir Casting



## Theoretical Calculations

### Introduction

- Composites consist of Reinforcement and Matrix phase.
- Mechanical properties of these composites depend on the volume fraction of reinforcement and matrix.
- The reinforcement material can be either fibre, particle, or whiskers.
- Reinforcement weight fraction can be measured practically to compute the reinforcement volume fraction.

Formula:

Weight of composite,  $W_c = W_f + W_m$

Weight of matrix,  $W_m = W_c - W_f$

For unit weight of composite,  $1 = W_f + W_m$

$W_c$  – Weight of Composite

$W_f$  – Weight of Fibre / Reinforcement

$W_m$  – Weight of Matrix

Void content is assumed to be negligible.

Table 3.3 Theoretical Calculations of work pieces volumes

volume ((170*75*45)/1000) cc	weight fractions(%)		
573.75	100	0	0
573.75	98	1	1
573.75	98	1	1
573.75	96	2	2
573.75	96	2	2
573.75	94	3	3
573.75	94	3	3
573.75	92	4	4

### Reinforcement Volume Fraction Formula

$$V_f = \frac{W_f / \rho_f}{(W_f / \rho_f) + (W_m / \rho_m)},$$

Where,

$V_f$  – Volume fraction of Fiber / Reinforcement

$V_m$  – Volume fraction of Matrix

$\rho_f$  – Density of Fiber / Reinforcement

$\rho_m$  – Density of matrix

$V_c$  – Volume fraction of Composite

Table 3.4 Theoretical calculations of volume fractions

VOLUME FRACTION		
MATRIX	REINFORCEMENT-1	REINFORCEMENT-2
1	0	0
0.988007986	0.004670769	0.007321245
0.988007986	0.004670769	0.007321245
0.975818375	0.0094185	0.014763125
0.975818375	0.0094185	0.014763125
0.96342624	0.014245112	0.022328648
0.96342624	0.014245112	0.022328648
0.950826494	0.019152587	0.030020919

### Density of composite

Volume of composite ,  $V_c = V_f + V_m$

For unit volume of composite,  $1 = V_f + V_m$

Volume fraction of matrix,  $V_m = 1 - V_f$

Density of composite,  $\rho_c = \rho_f V_f + \rho_m V_m$

Table 3.5 Composite density

density ( $\rho_c$ ) g/cc	mass kg	Mass of composite(adding slack) kg
1.83	1.0499625	1.15495875
1.844953689	1.058542179	1.164396397
1.844953689	1.058542179	1.164396397
1.860153777	1.067263229	1.173989552
1.860153777	1.067263229	1.173989552
1.875606404	1.076129174	1.183742092
1.875606404	1.076129174	1.183742092
1.891317918	1.085143655	1.193658021

Table 3.6 Masses of matrix and reinforcements

mass MATRIX gram	mass REINFORCEMENT1 gram	mass REINFORCEMENT 2 gram	Mass of composite
1154.95875	0	0	1154.95875
1141.108469	11.64396397	11.64396397	1164.396397
1141.108469	11.64396397	11.64396397	1164.396397
1127.02997	23.47979105	23.47979105	1173.989552
1127.02997	23.47979105	23.47979105	1173.989552
1112.717566	35.51226276	35.51226276	1183.742092
1112.717566	35.51226276	35.51226276	1183.742092
1098.165379	47.74632083	47.74632083	1193.658021

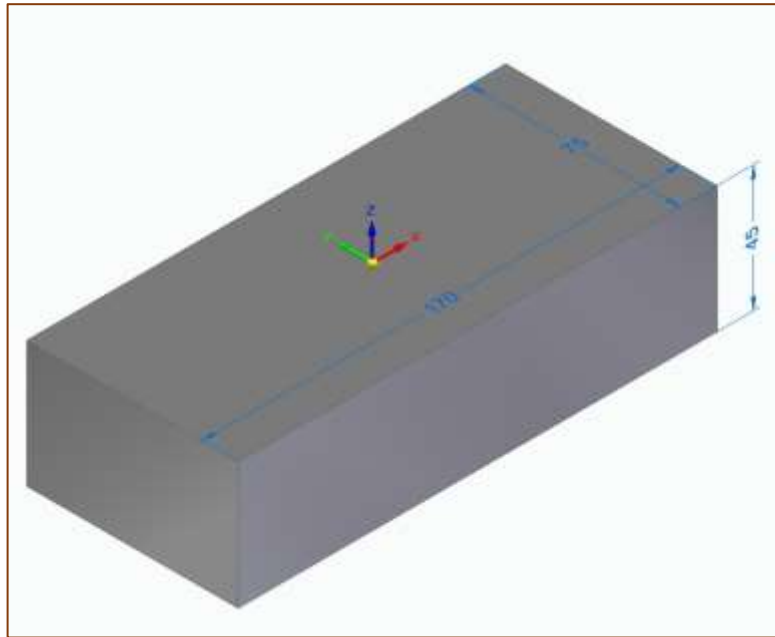


Fig.3.6 Work Piece 3d Model

### 3.2 Holes For Setting Vibrometer

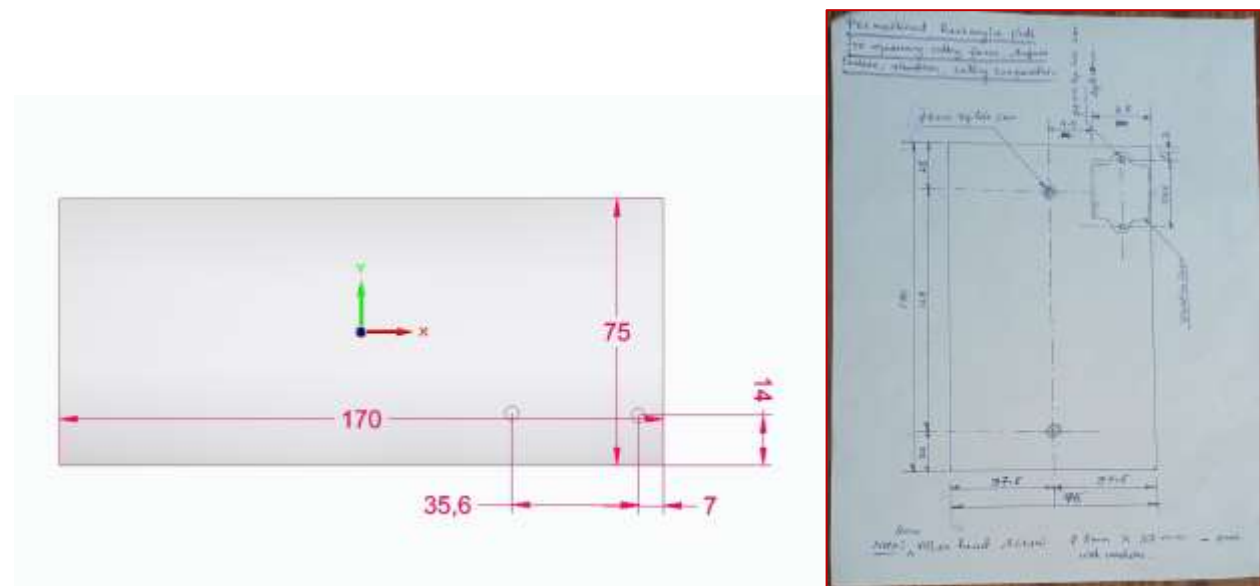


Fig.3.7 Planning for holes



<b>Material</b>	High Speed Steel, Alloy Steel
<b>Finish Type</b>	Black Oxide
<b>Cutting Angle</b>	135 Degrees
<b>Brand</b>	Bosch
<b>Item Dimensions L&amp;D</b>	75mm & 4mm

**Fig.3.8 Bosch Professional Twist Drill for making holes**



**Fig.3.9 Workpiece after making holes**

### 3.3 SDM(Surface Defect Machining)

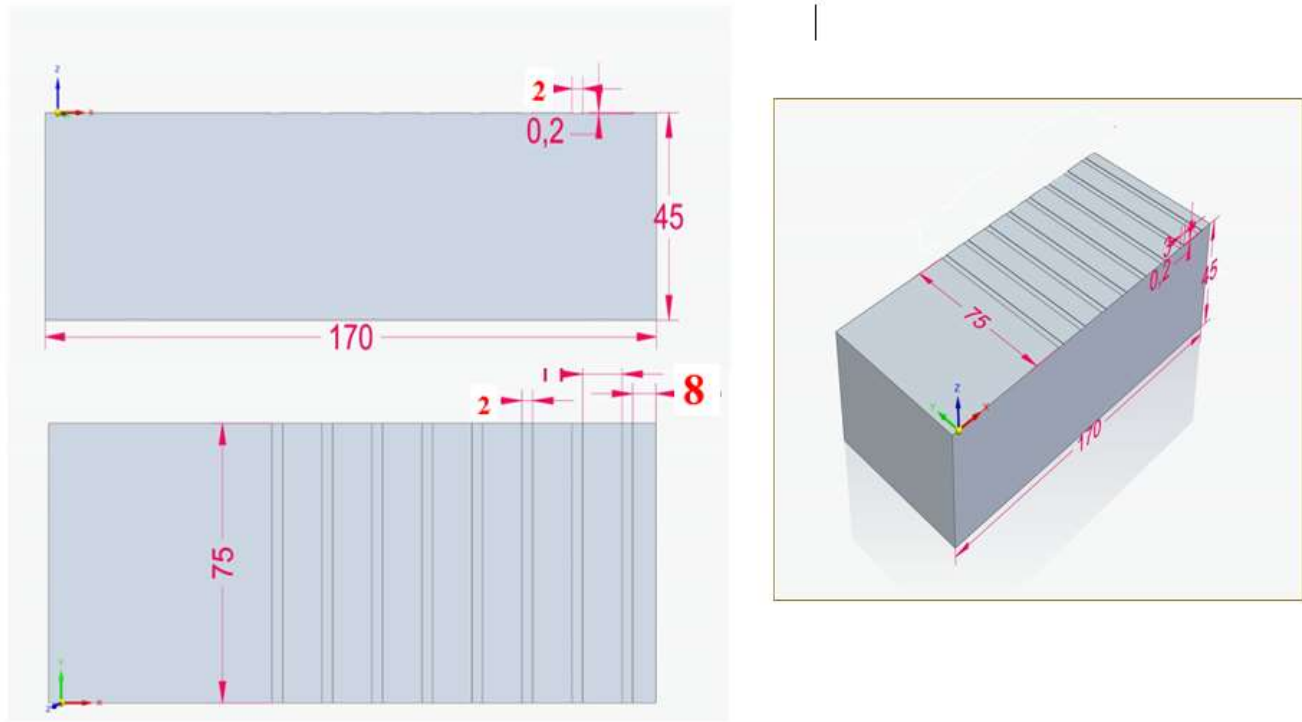


Fig.3.10 Planning for SDM



Fig.3.11 3-Axis CNC Milling Machine operated by SINUMERIK (808d,828d,840d)

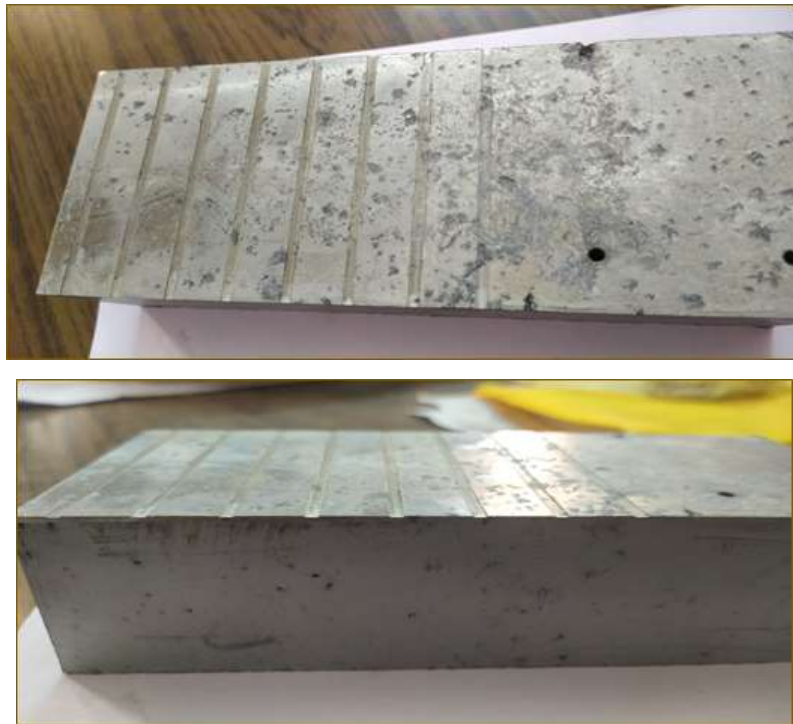


Fig.3.12 Workpiece after SDM

### 3.4 Experimentation

#### Design Of Experiments

MINITAB, STATISTICA, DESIGN EXPERT, etc. are software tools that can be used for experimental design and analyze data.

Response surface methodology (RSM) is a collection of mathematical and statistical techniques whose purpose is to analyze, by an empirical model, problems as the one posed.

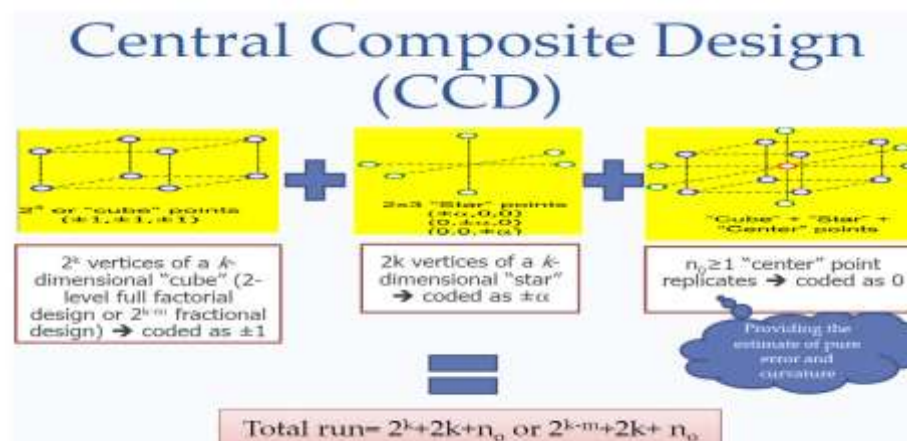


Table 3.7 Input variables

Factors	Level 1	Level 2	Level 3	Level 4	Level 5
Depth of cut	0.3 mm	0.45 mm	0.6 mm	0.75 mm	0.9 mm
speed of spindle	250 rpm	500 rpm	750 rpm	1000 rpm	1250 rpm
Feed	10 mm/min	20 mm/min	30 mm/min	40 mm/min	50 mm/min
Weight fractions	0 %	2 %	4 %	6 %	8 %

Based on weight fraction runs are

Table 3.8 Total 31 experiment

Weight Fraction	Experiments
0 %	1
2 %	8
4 %	13
6 %	8
8 %	1



### 3-AXIS Milling machine operated by siemens SINUMERIK 808d software



Fig.3.13 3-AXIS Milling machine

Table 3.9 3 axis Milling machine operated by siemens SINUMERIK 808d software

MANUFACTURER	BHARAT FRIETZ WERNER,BANGALORE
MODEL	BMV 40 T20
CNC CONTROL SYSTEM	SIEMENS 802D
TABLE SIZE	710mm*400mm
TRAVERSE (X,Y,Z)	510*410*460mm <sup>3</sup>
MAGAZINE CAPACITY	20 Tools
SPINDLE SPEED RANGE	60-6000 RPM
SPINDLE MOTOR	AC 10 Kw
TOTAL CONNECTED LOAD	25 KVA



Fig.3.14 Carbide 4 Flutes End Mills 12mm Diameter 75mm Length (CNC Milling Cutter)

### Vibrometer :

#### Specifications

- Pc based USB accelerometer
- Model : 7543A triaxial accelerometer
- Software : vibrascout software

#### Measurement range

- Displacement : 0.001 – 4.000 mm
- Velocity : 0.1 – 400.0 mm/sec
- Acceleration : 0.1 – 400.0 m/sec<sup>2</sup>
- make : USA

PC based USB Triaxial  
Accelerometer Adams  
Technologies /7543A



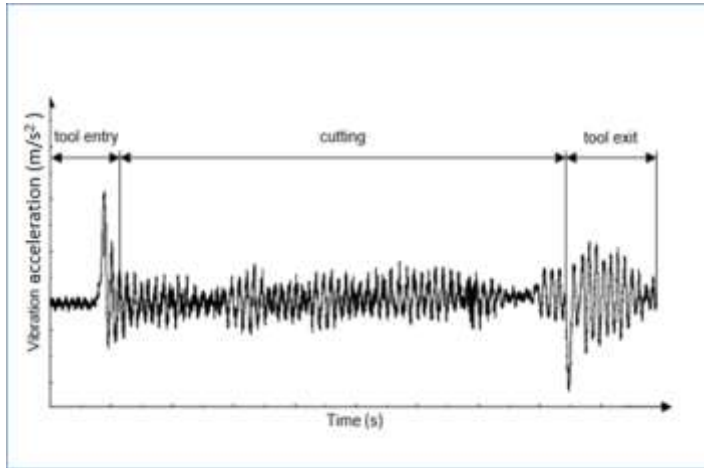
Fig.3.15 Vibrometer

### Vibration Measurement :

Using **VIBRASCOUT** software we are measuring the vibrations, that are produced on workpiece while cutting grooves with the carbide end mill.

**Vibration measured in cutting direction & tool spindle axis direction(X,Z axis).**

**Vibration acceleration amplitude.**



The signals captured by the sensors can be analyzed as a function of time or frequency. An example vibration acceleration signal waveform in the time domain is shown.

**Fig.3.16 Example Vibration Acceleration Signal Waveform In The Time Domain**

During the analysis of vibration displacement and acceleration, the amplitude was determined as half the difference between the maximum and minimum value, according to Equations.

$$Ax_y = \frac{(x_{y\_max} - x_{y\_min})}{2}$$

$$Aa_y = \frac{(a_{y\_max} - a_{y\_min})}{2}$$

where:  $Aa_y$ —acceleration amplitude,  $a_{y\_max}$ —maximum acceleration value,  $a_{y\_min}$ —minimum acceleration value.

## 4. RESULTS AND DISCUSSION

★ **Vibrations in Tool Axis Direction** → z-axis Acceleration Amplitude In  $\text{m/s}^2$

★ **Vibrations in Tool Movement Direction** → x-axis Acceleration Amplitude In  $\text{m/s}^2$

Table 4.1 **Results From Experimentation**

Run Order	Tool rotational speed (rpm)	Feed (mm/rev)	Depth of cut (mm)	% weight fraction	Z-axis Acceleration Amplitude( $\text{m/s}^2$ )	X-axis Acceleration Amplitude( $\text{m/s}^2$ )
1	500	20	0.45	6	10.08241	11.611055
2	750	30	0.3	4	14.683625	15.9884
3	1000	40	0.75	2	8.556784	9.37797
4	500	20	0.75	2	7.05979	11.3389
5	500	20	0.75	6	10.219527	10.448165
6	750	50	0.6	4	13.010295	17.35125
7	1000	40	0.45	2	11.162235	12.19235
8	500	40	0.75	6	10.86014	15.50525
9	750	30	0.6	4	20.11701	29.85605
10	1000	40	0.45	6	15.587035	18.8286
11	500	40	0.45	2	8.858835	19.8608
12	750	30	0.6	4	21.93635	25.06125
13	1000	20	0.75	6	13.92297	18.9107
14	1250	30	0.6	4	19.98471	25.6067
15	750	10	0.6	4	13.35557	17.9261
16	750	30	0.6	4	21.93635	25.06125
17	750	30	0.6	4	20.11701	29.85605
18	1000	20	0.45	2	9.752225	11.7613
19	750	30	0.6	4	21.93635	25.06125
20	750	30	0.6	0	9.05	12.35
21	500	40	0.75	2	9.182445	27.12655
22	1000	40	0.75	6	14.84115	20.78445
23	750	30	0.9	4	15.34006	19.3169

24	500	20	0.45	2	10.331401	13.132835
25	750	30	0.6	8	16.1225	15.93805
26	750	30	0.6	4	20.11701	29.85605
27	250	30	0.6	4	6.73836	9.194075
28	500	40	0.45	6	9.92738	16.70065
29	1000	20	0.45	6	16.163775	23.64955
30	1000	20	0.75	2	13.818755	21.71405
31	750	30	0.6	4	20.11701	29.85605

#### 4.1 Vibrations in Tool Axis Direction → z-axis Acceleration Amplitude In $\text{m/s}^2$

##### Response Surface Regression

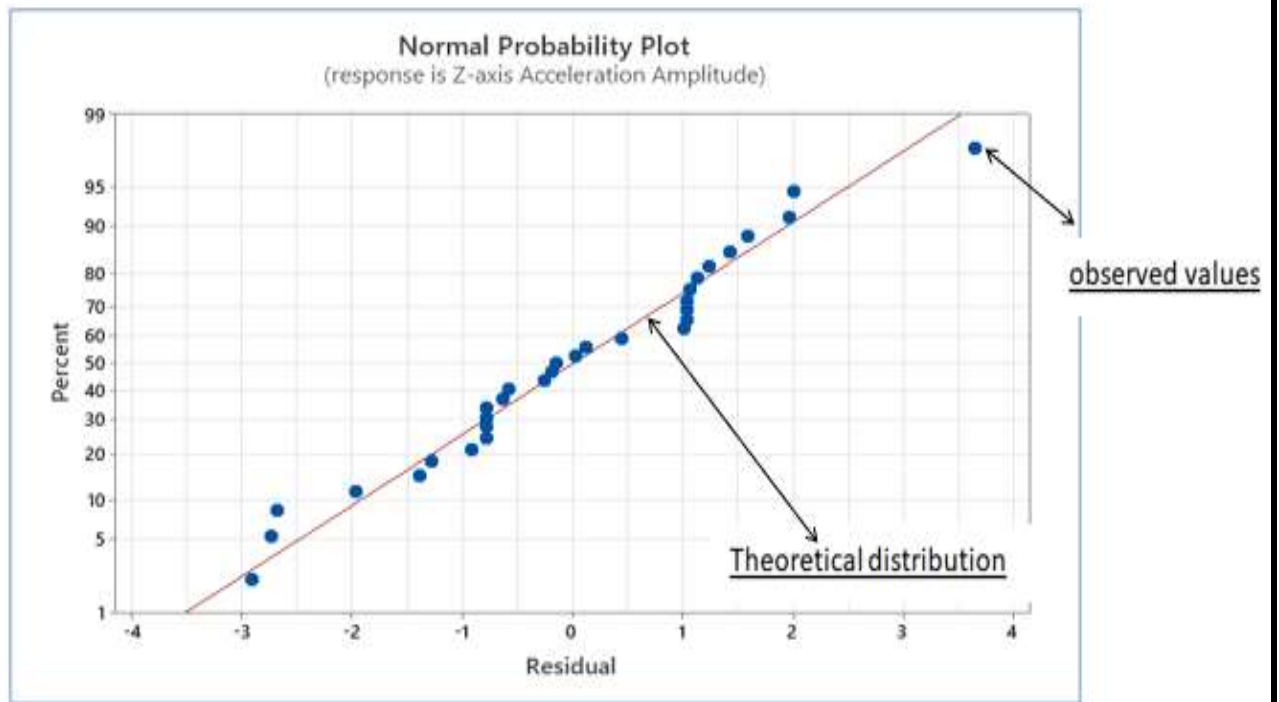


Fig.4.1 Normal probability plot (Z-axis Acceleration Amplitude)

##### Analysis of Variance

Table 4.2 Analysis of Variance (Z-axis Acceleration Amplitude)

Source	DF	Adj SS	Adj MS	F-Value	P-Value	% of influence
Model	14	647.297	46.236	10.74	0.000	90.38
Linear	4	178.191	44.548	10.35	0.000	24.88
Tool rotational speed	1	120.493	120.493	27.98	0.000	16.82
Feed	1	0.392	0.392	0.09	0.767	0.05
Depth of cut	1	0.182	0.182	0.04	0.840	0.02
% weight fraction	1	57.125	57.125	13.27	0.002	7.97
Square	4	458.321	114.580	26.61	0.000	63.99
Tool rotational speed*Tool rotational speed	1	154.751	154.751	35.94	0.000	21.60
Feed*Feed	1	160.749	160.749	37.33	0.000	22.44
Depth of cut*Depth of cut	1	104.728	104.728	24.32	0.000	14.62

% weight fraction*% weight fraction	1	181.612	181.612	42.18	0.000	25.35
2-Way Interaction	6	10.785	1.798	0.42	0.857	1.50
Tool rotational speed*Feed	1	1.349	1.349	0.31	0.583	0.18
Tool rotational speed*Depth of cut	1	0.008	0.008	0.00	0.967	0.001
Tool rotational speed*% weight fraction	1	8.364	8.364	1.94	0.182	1.16
Feed*Depth of cut	1	0.039	0.039	0.01	0.926	0.005
Feed*% weight fraction	1	1.014	1.014	0.24	0.634	0.14
Depth of cut*% weight fraction	1	0.012	0.012	0.00	0.959	0.001
Error	16	68.895	4.306			9.61
Lack-of-Fit	10	63.221	6.322	6.69	0.015	8.82
Pure Error	6	5.674	0.946			0.79
Total	30	716.192				100

#### NOTE

It shows that in this model the influence of square source is more, and in linear source tool rotational speed, in square source % weight fraction \* % weight fraction, in 2 way interactions tool rotational speed\*% weight fraction are influence output vibration. The error/residual total 10%, in that lack of fit is 9.15% remaining pure error.

#### Model Summary

Table 4.3 Model Summary (Z-axis Acceleration Amplitude)

S	R-sq	R-sq(adj)	R-sq(pred)
2.07508	90.03%	81.30%	46.17%

R-sq is closer to 1, the predicted model is more reliable.

R -sq >0.75 acceptable, however, >0.8 is much better.

#### Coefficients



Table 4.4 Coefficients (Z-axis Acceleration Amplitude)

Term	Coef	SE Coef	T-Value	P-Value	significant
Constant	20.897	0.784	26.64	0.000	
Tool rotational speed	2.241	0.424	5.29	0.000	✓
Feed	-0.128	0.424	-0.30	0.767	
Depth of cut	-0.087	0.424	-0.21	0.840	
% weight fraction	1.543	0.424	3.64	0.002	✓
Tool rotational speed*Tool rotational speed	-2.261	0.388	-5.83	0.000	✓
Feed*Feed	-2.306	0.388	-5.94	0.000	✓
Depth of cut*Depth of cut	-1.849	0.388	-4.76	0.000	✓
% weight fraction*% weight fraction	-2.455	0.388	-6.33	0.000	✓
Tool rotational speed*Feed	-0.290	0.519	-0.56	0.583	
Tool rotational speed*Depth of cut	0.022	0.519	0.04	0.967	
Tool rotational speed*% weight fraction	0.723	0.519	1.39	0.182	
Feed*Depth of cut	-0.049	0.519	-0.09	0.926	
Feed*% weight fraction	0.252	0.519	0.49	0.634	
Depth of cut*% weight fraction	-0.027	0.519	-0.05	0.959	

NOTE : It shows that based on p values linear terms of tool rotational speed and % weight fraction are significant and all square terms are significant.

## Main Effects Plot

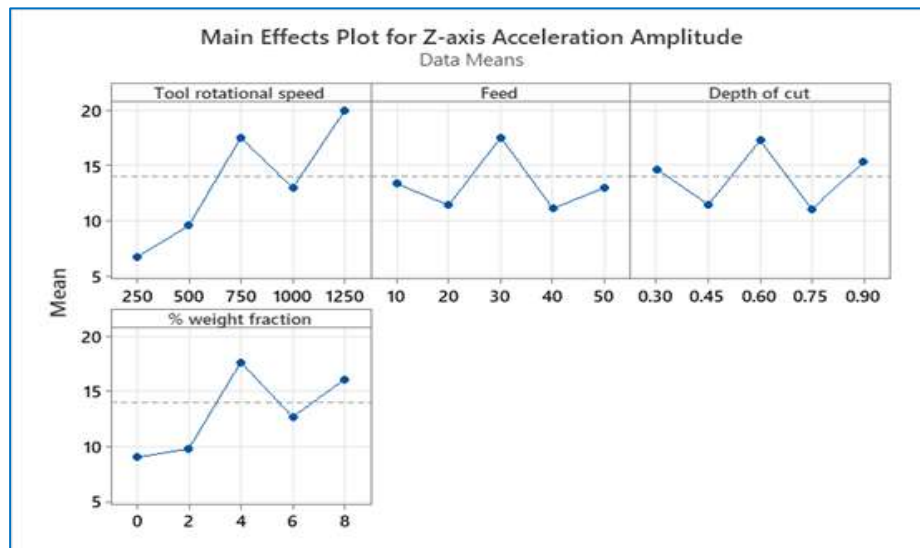


Fig.4.2 Main Effect Plot (Z-axis Acceleration Amplitude)

NOTE: It shows that the Acceleration amplitude of vibration is increases with increasing the tool rotational speed and %weight fraction.

## Interactions Plot

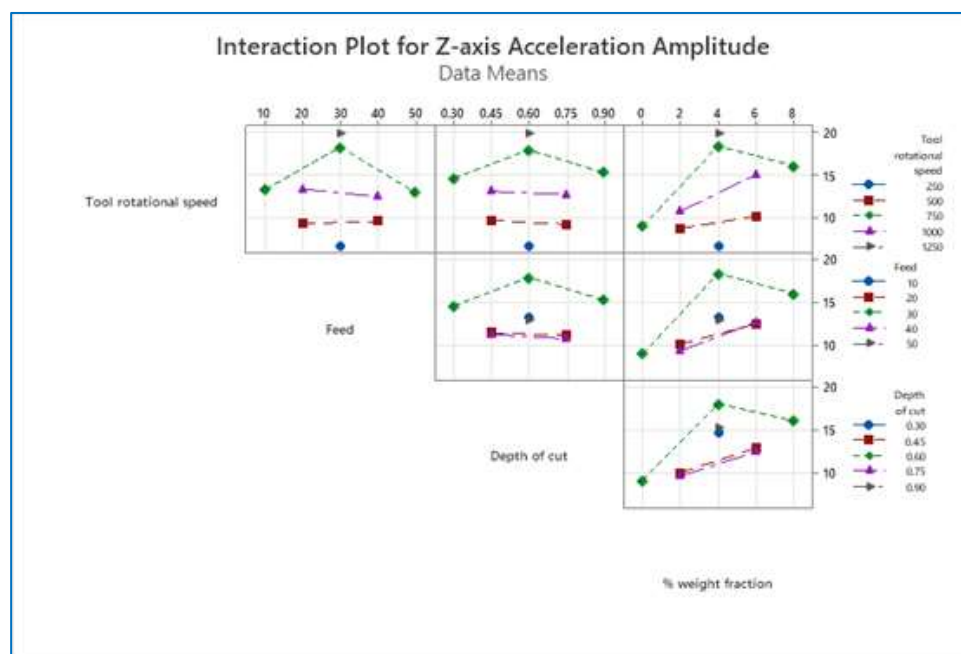


Fig.4.3 Interaction Plot (Z-axis Acceleration Amplitude)

NOTE: It shows that good interaction is find in **%weight fraction vs depth of cut** and **Feed vs %weight fraction**.

### Regression Analysis

#### Regression Equation

Z-axis Acceleration Amplitude	=	$4.95 + 0.00896 \text{ Tool rotational speed} - 0.0128 \text{ Feed}$ $- 0.58 \text{ Depth of cut} + 0.771 \% \text{ weight fraction}$
-------------------------------------	---	---

1. R-sq - Coefficient of Determination
2. R - Coefficient of Correlation
3. SSR - Sum of squares of regression
4. SST - Total variation of the observed values of activity

$$R^2 = SSR/SST$$

$$\text{adj } R^2 = 1 - \text{MS}_{\text{residual}} / (\text{SST}/N)$$

R-sq is closer to 1, the predicted model is more reliable.

**R -sq>0.75 acceptable , however, >0.8 is much better**

★ **F-value** = MS regression/MS residual

★ **T-value** = coefficient/ standard error

★ **P-value**

Can be visualized.

- Pareto Chart
- Normal Probability

If a p-value is  $\leq 0.01$  - “convincing”

$0.01 < \text{p-value} \leq 0.05$ , - “strong”

$0.05 < \text{p-value} \leq 0.10$  - “Gray area/moderate”

p-value  $> 0.10$  - “weak” or “no”

## 4.2 Vibrations in Tool Movement Direction → X-axis Acceleration Amplitude In $\text{m/s}^2$

### Response Surface Regression

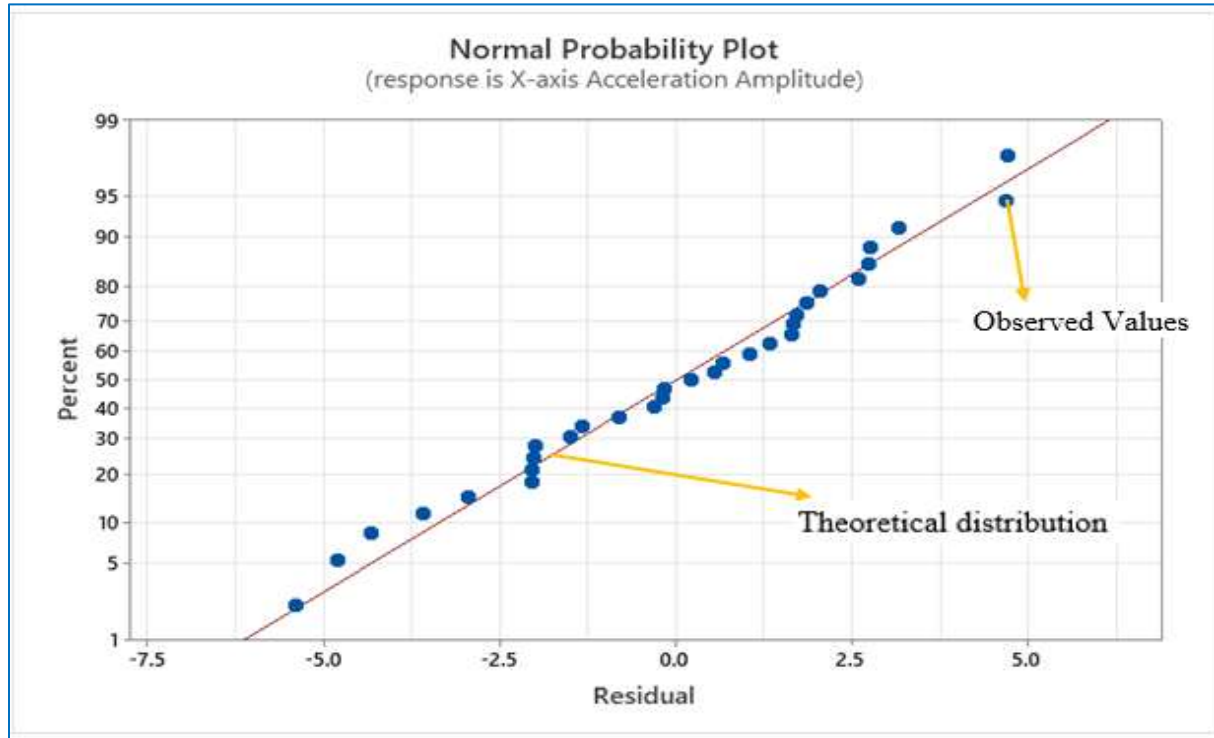


Fig.4.4 Normal probability plot (X-axis Acceleration Amplitude)

### Analysis of Variance

Table 4.5 Analysis of Variance (X-axis Acceleration Amplitude)

Source	DF	Adj SS	Adj MS	F-Value	P-Value	% of influence
Model	14	1021.60	72.972	5.56	0.001	82.93
Linear	4	113.92	28.480	2.17	0.119	9.24
Tool rotational speed	1	81.84	81.844	6.23	0.024	6.64
Feed	1	11.57	11.565	0.88	0.362	0.93
Depth of cut	1	8.31	8.314	0.63	0.438	0.67
% weight fraction	1	12.20	12.198	0.93	0.350	0.99
Square	4	622.74	155.685	11.85	0.000	50.55
Tool rotational speed*Tool rotational speed	1	174.30	174.298	13.27	0.002	14.15
Feed*Feed	1	165.99	165.988	12.64	0.003	13.47

Depth of cut*Depth of cut	1	165.51	165.507	12.60	0.003	13.43
% weight fraction*% weight fraction	1	308.20	308.197	23.47	0.000	25.02
2-Way Interaction	6	284.94	47.490	3.62	0.018	23.13
Tool rotational speed*Feed	1	141.10	141.102	10.74	0.005	11.45
Tool rotational speed*Depth of cut	1	0.10	0.096	0.01	0.933	0.008
Tool rotational speed*% weight fraction	1	122.78	122.775	9.35	0.008	9.96
Feed*Depth of cut	1	0.55	0.546	0.04	0.841	0.044
Feed*% weight fraction	1	0.73	0.727	0.06	0.817	0.059
Depth of cut*% weight fraction	1	19.69	19.695	1.50	0.238	1.59
Error	16	210.14	13.134			17.06
Lack-of-Fit	10	171.68	17.168	2.68	0.120	13.93
Pure Error	6	38.46	6.411			3.12
Total	30	1231.75				100

## NOTE

It shows that in this model the influence of square source is more, and in linear source **tool rotational speed**, In square source **% weight fraction\*% weight fraction**, In 2 way interactions **Tool rotational speed\*Feed** are influence output vibration. The error/residual total 17%, in that lack of fit is 14% & remaining pure error.

## Model Summary

Table 4.6 Model Summary (X-axis Acceleration Amplitude)

S	R-sq	R-sq(adj)	R-sq(pred)
3.62406	83.00%	68.01%	15.47%

R-sq is closer to 1, the predicted model is more reliable.

R -sq>0.75 acceptable , however, >0.8 is much better.

## Coefficients

Table 4.7 Coefficients (X-axis Acceleration Amplitude)

Term	Coef	SE Coef	T-Value	P-Value	significant
Constant	27.09	1.37	19.78	0.000	
Tool rotational speed	1.847	0.740	2.50	0.024	✓
Feed	0.694	0.740	0.94	0.362	
Depth of cut	0.589	0.740	0.80	0.438	
% weight fraction	0.713	0.740	0.96	0.350	
Tool rotational speed*Tool rotational speed	-2.469	0.678	-3.64	0.002	✓
Feed*Feed	-2.409	0.678	-3.56	0.003	✓
Depth of cut*Depth of cut	-2.406	0.678	-3.55	0.003	✓
% weight fraction*% weight fraction	-3.283	0.678	-4.84	0.000	✓
Tool rotational speed*Feed	-2.970	0.906	-3.28	0.005	✓
Tool rotational speed*Depth of cut	0.078	0.906	0.09	0.933	
Tool rotational speed*% weight fraction	2.770	0.906	3.06	0.008	
Feed*Depth of cut	0.185	0.906	0.20	0.841	
Feed*% weight fraction	-0.213	0.906	-0.24	0.817	
Depth of cut*% weight fraction	-1.109	0.906	-1.22	0.238	

NOTE : It shows that based on p values linear terms of tool rotational speed and % weight fraction are significant and all square terms are significant.

**Main Effect Plot**



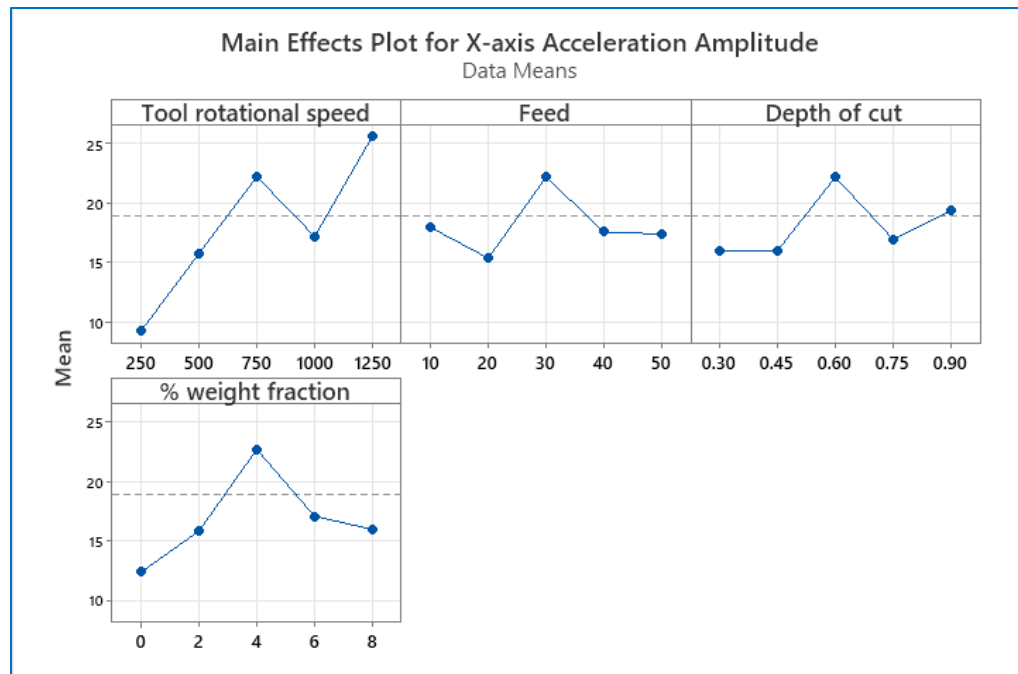


Fig.4.5 Main Effects Plot (X-axis Acceleration Amplitude)

NOTE : It shows that the Acceleration amplitude of vibration is increases with increasing the tool rotational speed.

### Interaction Plot

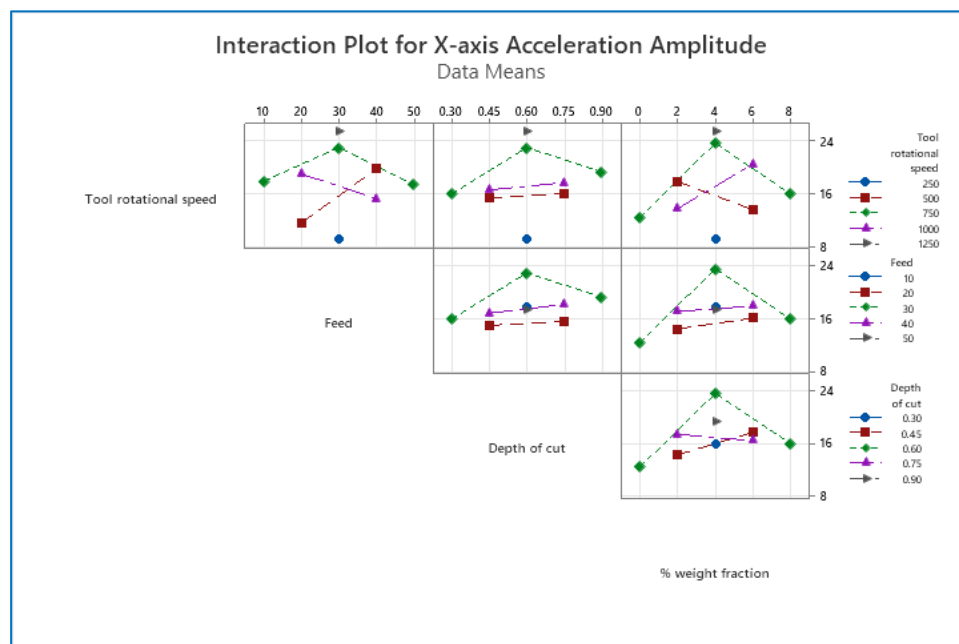


Fig.4.6 Interaction Plot (X-axis Acceleration Amplitude)

NOTE : It shows that good interaction is find in %weight fraction vs depth of cut and %weight fraction vs Feed.

## Regression Analysis

### Regression Equation

X-axis Acceleration Amplitude	=	$7.51 + 0.00739 \text{ Tool rotational speed} + 0.069 \text{ Feed}$ $+ 3.92 \text{ Depth of cut} + 0.356 \% \text{ weight fraction}$
-------------------------------	---	---

## **5. CONCLUSION**

### **5.1 Vibrations in Tool Axis Direction → Z-Axis Acceleration Amplitude In $\text{m/s}^2$**

- ★ ANOVA data explain that the Vibration acceleration amplitude is clearly influenced by the tool rotational speed and %weight fraction, and they are also strong significant values. The influence of feed rate & depth of cut on Vibration acceleration amplitude cannot be clearly demonstrated.
- ★ Main Effects Plot explain that the Vibration amplitude increases with an increase in spindle speed and % weight fraction. The Vibrations acceleration amplitude optimum at 250 rpm tool rotational speed, 10 mm/min feed, 0.75 mm depth of cut and 0% weight fraction.

### **5.2 Vibrations in Tool Movement Direction → x-axis Acceleration Amplitude In $\text{m/s}^2$**

- ★ ANOVA data explain that the Vibration acceleration amplitude is clearly influenced by the tool rotational speed and, and they are also strong significant values. The influence of feed rate & depth of cut on Vibration acceleration amplitude cannot be clearly demonstrated.
  - ★ Main Effects Plot explain that the Vibration amplitude increases with an increase in spindle speed. The Vibrations acceleration amplitude optimum at 250 rpm tool rotational speed, 20 mm/min feed, 0.3 mm and 0.45 mm depth of cut and 0% weight fraction.
-

## 6. REFERENCES

1. YasharBehnamian,Dominic Serate, Ermia Aghaie, RaminZahiri , ZacharyTolentino, HamidNiazi, AmirMostafaeid (2021)“Tribological behavior of ZK60 magnesium matrix composite reinforced by hybrid MWCNTs/B4C prepared by stir casting method” Department of Chemical and Materials Engineering, University of Alberta, Edmonton, Alberta T6G 2V4.
2. Y.V.R.K.Prasad, K.P.Rao, M.Gupta(2008), “Hot workability and deformation mechanisms in Mg/nano–Al<sub>2</sub>O<sub>3</sub> composite”, Department of Manufacturing Engineering and Engineering Management, City University of Hong Kong, Tat Chee Avenue, Kowloon, Hong Kong SAR, China.
3. Muhammad Owais Qadri and Hamidreza Namazi (2020) “Fractal-based analysis of the relation between surface finish and machine vibration in milling operation”, Fluctuation and Noise Letters Vol. 19, No. 01, 2050006.
4. Md Sayem Hossain Bhuiyan and Imtiaz Choudhury,(2015)”Investigation of tool wear and surface finish by analyzing vibration signals in turning Assab-705 steel” Machining Science and Technology 19(2):236-261.
5. Wencai Liu, Jie Dong, Ping Zhang, Chunquan Zhai and Wenjiang Ding,“Effect of Shot Peening on Surface Characteristics and Fatigue Properties of T5-Treated ZK60 Alloy “,National Engineering Research Center of Light Alloy Net Forming, School of Materials Science and Engineering,Shanghai Jiao Tong University, Shanghai 200240, P.R.China.
6. Sukhdev S. Bhogal, Charanjeet Sindhu,Sukhdeep S. Dhami and B. S. Pabla (2014)“Minimization of surface roughness and tool vibration in CNC milling operation.”,National Institute of Technical Teachers and Training, Chandigarh 160019, India.

7. Yung-Chih Lin ,Kung-Da Wu 1,Wei-Cheng Shih Pao-Kai Hsu and Jui-Pin Hung  
“Prediction of Surface Roughness Based on Cutting Parameters and Machining Vibration  
in End Milling Using Regression Method and Artificial Neural Network” .
8. Justin Aral Gonsalves, Sadvidya N. Nayak, Gururaj Bolar (2020),“Experimental  
investigation on the performance of helical milling for hole processing in AZ31  
magnesium alloy”.
9. Kaining Shi, Dinghua Zhang, Junxue Ren, Changfeng Yao and Xinchun Huang(2015),  
“Effect of cutting parameters on machinability characteristics in milling of magnesium  
alloy with carbide tool”.
10. Yanhua Zhaoa, Jie Suna,, Jianfeng (2014) “Effect of rare earth oxide on the properties of  
laser cladding layer and machining vibration suppressing in side milling”.
11. S. Jayasathyakawin , M. Ravichandran , N. Baskar , C. Anand Chairman , R.  
Balasundaram(2019) “Mechanical properties and applications of Magnesium alloy –  
Review”, Anna University, Chennai 600 025, India.
12. Navneet Khanna & Prassan Shah1 & Narendra Mohan Suri & Chetan Agrawal1 &  
Sandeep K. Khatkar & Franci Pusavec & Murat Sarikaya, (2020), “Application of  
Environmentally-friendly Cooling/Lubrication Strategies for Turning Magnesium/SiC  
MMCs”.
13. Ireneusz Zagórski , Jarosław Korpysa and Andrzej Weremczuk (2021) “Influence of Tool  
Holder Types on Vibration in Rough Milling of AZ91D Magnesium Alloy”.
14. K. Weinert,( 1993) ,“A Consideration of Tool Wear Mechanism when Machining Metal  
Matrix Composites (MMC)”.
15. Thomas Friemuth and Jens Winkler, “Machining of Magnesium Workpieces”.

16. J. Z. Hou, Wei Zhou, and N. Zhao, (2010)” Effect of Cutting Parameters on Ignition of AM50A Mg Alloy during Face Milling”.
17. Liwei Lu , Shaohua Hu, Longfei Liu , Zhenru Yin (2016) “High-speed cutting of AZ31 magnesium alloy”.
18. Junzhan Hou , Ning Zhao & Shaoli Zhu (2011),” Influence of Cutting Speed on Flank Temperature during Face Milling of Magnesium Alloy”

#### BOOK

19. MAGNESIUM, MAGNESIUM ALLOYS , AND MAGNESIUM COMPOSITES  
Manoj Gupta, Nai Mui Ling Sharon.

#### WEBSITE

20. <https://www.intechopen.com/chapters/58816>.
-